

Ammonia excretion in the freshwater planarian

Schmidtea mediterranea

^{§*}Dirk Weihrauch, [§]Ainsely C. Chan, [£]Heiko Meyer, [£]Carmen Döring, [§]Mary Sourial, and
[§]Michael J. O'Donnell

* Corresponding author, [§]Department of Biological Sciences, University of Manitoba, Winnipeg, MB,
R3T2N2, Canada; [£] Department of Zoology/Developmental Biology, University of Osnabrück, ,
Osnabrück, Germany; [§]Department of Biology, McMaster University, Hamilton, ON, L8S 4K1, Canada

Key words: Ammonia excretion, Rh-protein, *Schmidtea mediterranea*, HEA

Abstract

In aquatic invertebrates metabolic nitrogenous waste is excreted predominately as ammonia. Very little is known, however, of the underlying mechanisms of ammonia excretion, particularly in freshwater species. Our results indicate that in the non-parasitic freshwater planarian *Schmidtea mediterranea* ammonia excretion depends on an acidification of the apical unstirred layer of the body surface and consequent ammonia trapping. Buffering of the environment to a pH of 7 or higher decreased excretion rate. Inhibitor experiments suggested further that the excretion mechanism involves the participation of the V-type H⁺-ATPase and carbonic anhydrase and possibly also the Na⁺/K⁺-ATPase and Na⁺/H⁺ exchangers (NHEs). Alkalinization (pH 8.5, 2 days) of the environment led to a 1.9-fold increase in body ammonia levels and to a down-regulation of V-ATPase (subunit A) and Rh-protein mRNA. Further, a two day exposure to non-lethal ammonia concentrations (1 mmol L⁻¹) caused a doubling of body ammonia levels and led to an increase in Rh-protein and Na⁺/K⁺-ATPase (α -subunit) mRNA expression levels. *In-situ* hybridization studies indicated a strong mRNA expression of the Rh-protein in the epidermal epithelium. The ammonia excretion mechanism proposed for *S. mediterranea* reveals striking similarities to the current model suggested to function in gills of freshwater fish.

Introduction

Ammonia is an end product of amino acid metabolism but it can also be produced by ureolytic and uricolytic pathways. In this study, NH_3 refers to gaseous ammonia, NH_4^+ to ammonium ions, and ammonia to the sum of both. Ammonia is a weak base (pK = 9.2 to 9.8) and occurs in solutions in a pH-dependent equilibrium of uncharged, membrane permeable NH_3 and ionic NH_4^+ (Cameron and Heisler, 1983). Although produced by essentially all cells, ammonia causes a number of toxic effects in animal systems. Likely most severe are the effects of ammonia on the central nervous system as reported extensively for mammalian systems. Here ammonia causes swelling and cell death of astrocytes (Butterworth, 2002; Ip and Chew, 2010) and excessive activation of *N*-methyl-D-aspartate (NMDA)-type glutamate receptors (Marcaida et al., 1992). Ammonia has further direct inhibitory effect on the astrocytic EAAT-1 (GLAST) and EAAT-2 (GLT-1) transporters which are responsible for the removal of glutamate from the neuronal synapse (Chan et al., 2000; Knecht et al., 1997; Norenberg et al., 1997). Very high mRNA expression levels of Rh-like ammonia transporters observed in the ganglia of tobacco hornworm *Manduca sexta* (Weihrauch, 2006) and the fruitfly *Drosophila melanogaster* (FlyAtlas; (Chintapalli et al., 2007)) suggest that cells in the central nervous system of invertebrates also require a capacity to transport ammonia.

Due to its toxic effects ammonia must be rapidly excreted or metabolized to less toxic substances to keep its concentration in the body fluids in a tolerable range. With the exception of mammals and elasmobranchs, the vast majority of aquatic living species, including fully aquatic amphibia (Cragg et al., 1961; Fanelli and Goldstein,

1964; Wood et al., 1989), teleost fish (Weihrauch et al., 2009; Wright and Wood, 2009) , and virtually all aquatic invertebrates (Wright, 1995) are ammonotelic, excreting the majority of their nitrogenous waste directly as ammonia.

Excretion usually occurs across gas exchanging or ionoregulatory epithelia, such as the gills (Potts, 1965; Weihrauch et al., 2004b; Weihrauch et al., 2009; Wilson et al., 1994; Wright and Wood, 2009), anal papillae (Donini and O'Donnell, 2005) or the skin (Fanelli and Goldstein, 1964; Shih et al., 2008). However, very little is known about the actual excretion mechanisms. With the discovery by Marini and coworkers that members of the Rhesus family function as ammonia transporters (Marini et al., 2000) this field of research gained considerable momentum over the last decade. The majority of studies focusing on ammonia excretion mechanisms in aquatic species were performed on decapod crustaceans and fish, as reviewed by Weihrauch and coworkers for crustaceans (Weihrauch et al., 2004b; Weihrauch et al., 2009) and by Wright and Wood for fish (Wright and Wood, 2009).

In crustaceans such as the green shore crab *Carcinus maenas*, branchial ammonia excretion is an active process, involving the basolateral Na^+/K^+ -ATPase, an intracellular (vesicular) H^+ -ATPase (V-ATPase), a functional microtubule system and likely also Rh-like ammonia transporters and apical cation/ H^+ exchangers (Lucu et al., 1989; Martin et al., 2011; Weihrauch et al., 1998; Weihrauch et al., 2004b; Weihrauch et al., 2002)

In contrast to the ammonia excretion modus in brackish and marine crabs, branchial ammonia excretion in freshwater fish depends on an acidification of the unstirred boundary layer on the apical surface of the gill (Weihrauch et al., 1998; Wilson et al., 1994). Ammonia from the blood appears to enter the pavement cell cytoplasm via

the Na⁺/K⁺-ATPase and a basolateral isoform of the Rh-like ammonia transporter, Rhbg. It is further proposed that an apical V-ATPase, perhaps in concert with NHE2, causes a local acidification of the gill boundary layer, thereby lowering the partial pressure of NH₃ (P_{NH_3}). The resulting partial pressure gradient of ammonia (ΔP_{NH_3}) across the apical membrane thus drives cellular NH₃ into the environment via a second Rh-protein, Rhcg2. Protons to fuel the V-ATPase/NHE are provided by the activity of an intracellular carbonic anhydrase (Nawata et al., 2007; Nawata and Wood, 2008; Nawata and Wood, 2009; Nawata et al., 2010b).

Mechanistic studies on ammonia excretion mechanisms in aquatic invertebrates other than crustaceans are very sparse. The present study provides the first insights into the ammonia excretion mechanisms in *Schmidtea mediterranea*. This carnivorous freshwater planarian of the phylum Platyhelminthes has recently become an important model system for the investigation of regeneration and stem cell biology (Sanchez Alvarado and Tsonis, 2006), but very little is known of its physiology. The epidermis of the planarian consists of a monostратified epithelium which is multiciliated on the ventral side. Mucus secreting gland cells (rhabdites) are located between the epithelial cells of the epidermis (Rompolas et al., 2009; Stevenson and Beane, 2010). Excretion experiments, together with gene expression analysis and *in-situ* hybridization studies, provide the first evidence that a freshwater invertebrate organism excretes ammonia via the epidermis in a manner similar to that proposed for branchial excretion in freshwater fish.

Methods

Animals

Schmidtea mediterranea were kept at room temperature under natural light settings in ca. 6 liter dechlorinated tap water per g fresh weight (FW). Water was aerated by means of an air stone and animals were fed once per week with small pieces of bovine liver. After feeding the tank water was replaced. Ammonia levels in the tanks were monitored on a regular basis and varied between 3 and 15 $\mu\text{mol L}^{-1}$ total ammonia. All animals were starved for 2 days before experimentation. All experiments were performed at room temperature during daylight.

Whole Body Excretion experiments

For all whole body excretion experiments a number of animals (ca. 0.1-0.15 g FW, ≥ 0.5 cm in length) were transferred into small glass containers (diameter = 2.5 cm, depth = 2 cm) filled with 4 ml of dechlorinated tap water. After an equilibration period of 0.5 hours, the water was replaced with 4 ml of fresh water for the first sampling period. Each sampling period lasted 1 hour. At the end of each sampling period, two samples of 1.9 ml were taken from the container for later analysis of water ammonia. Before each experimental step animals were rinsed by adding and draining 8 ml of dechlorinated tap water into and from the container, respectively.

Feeding experiments

In another series of experiments a feeding period (bovine liver, *ad libitum*) of 1 hour followed the control measurement (see above). To avoid stressful animal transfer, feeding took place in the experimental container, filled with 8 ml water. After a rinse of the experimental container with 8 ml of dechlorinated tap water, 4 ml of dechlorinated ammonia free tap water was added (see above) and the first sampling period after feeding followed, which lasted for one hour. Similar to the first sampling period, including a washing step 4 consecutive one-hour sampling followed. After these five consecutive one-hour sampling periods in ammonia free water the glass containers, which contained a pool of individual of animals (total mass = 0.15-0.25 g), were covered with a plastic mesh and were then placed into a 6 liter tank of dechlorinated tap water (aerated and ventilated by several air stones) until the final measurement that took place 16 hours after feeding. The mesh allowed free water exchange but not the passage of the animals. Samples were sealed and immediately frozen at -80 °C for later analysis of total ammonia, usually within 1 week.

Excretion experiments in various pH regimes

In experiments to determine excretion rates in pH-buffered media, a control sampling period in dechlorinated, non-buffered tap water (1 hour, pH= 8.3) was followed by a rinse and one experimental sampling period (1 hour) employing water buffered to one particular pH with either 10 mmol L⁻¹ 2-(*N*-morpholino)ethanesulfonic acid (MES) (for a pH of 5, 5.5 or 6), 2-(4-(2-hydroxyethyl)-1-piperazineethanesulfonic acid) (HEPES) (for a pH of 6.5, 7 or 7.5), or 2-Amino-2-hydroxymethyl-propane-1,3-diol

(TRIS Base) (for a pH of 8 and 8.5). Experimental solutions were finally adjusted with HCl or NaOH to the experimental pH.

Excretion experiments under the influence of varying inhibitors and after short-term exposure to various ammonia concentrations

In experiments to determine excretion rates under the influence of an inhibitor, a control sampling period employing dechlorinated, non-buffered tap water (1 hr, pH= 8.3) was followed by a rinse and a 30 minute pre-incubation period in media containing the inhibitor. A rinse was followed by a one hour experimental sampling period. Inhibitors were purchased from Sigma-Aldrich (St. Louis, MO, USA) and were prepared, with the exception of colchicine, at a concentration range known to be effective in other invertebrates (Blaesse et al., 2010; Onken and McNamara, 2002; Weihrauch et al., 2004a). The concentrations (in brackets) were: concanamycin C (5 $\mu\text{mol L}^{-1}$), acetazolamide (1 mmol L^{-1}), amiloride hydrochloride hydrate (10 mmol L^{-1}), ouabain (1 mmol L^{-1}), and colchicine (10 mmol L^{-1}). Amiloride hydrochloride hydrate and concanamycin C were dissolved in dimethyl sulfoxide (DMSO) at a final concentration of 0.5%. In these experiments 0.5% DMSO was also added to the control solutions.

In a series of experiments animals were exposed after an initial control sampling period for 1 hour to different environmental ammonia concentrations (0.1, 0.2, 0.5, 1, 5 and 10 mmol L^{-1} NH_4Cl ; $n \geq 5$ for all treatments). After exposure this short-time ammonia exposure, ammonia excretion rates were measured in ammonia free water consecutively over a period of 4 hours.

At the end of each experiment, animals were dried between paper towels, weighed and placed in a separate tank for a monitoring period of 7 days. Only if animals survived the monitoring period after any given treatment were the collected samples used for analysis. The samples were analyzed for their content of total ammonia on the day of experimentation or were sealed and immediately frozen at $-80\text{ }^{\circ}\text{C}$ for later analysis, usually within 1 week.

Long term pH and HEA exposure experiments

For long term exposure experiments, groups of animals (*ca.* 1 g FW in 2 liter) were kept for 48 hours either in a particular concentration of NH_4Cl (0.1, 0.2, 0.5, 1, 5, 10 mmol L^{-1} , not buffered, adjusted to pH 8.3) or in dechlorinated tap water buffered with 10 mmol L^{-1} MES (pH 5.5) HEPES (pH 7) or TRIS Base (pH 8.5). Experimental solutions were adjusted with HCl or NaOH to the experimental pH. After 24 hours the experimental solutions were refreshed. Tissue collection for analysis followed after total exposure time of 48 hours.

Ammonia concentration of animal tissue

For measurements of whole body ammonia concentration, animals were carefully dried between paper towels and weighed. A pool of animals from a certain treatment with a total fresh weight (FW) of approximately 0.1 g was placed in 1 ml of de-ionized water and homogenized on ice for 15 seconds using a polytron homogenizer (AHS, Pro Scientific Inc, Oxford, CT, USA). Immediately after homogenization the pH of the homogenate was determined followed by an addition of 3 ml of ice cold de-ionized water

enriched with $5 \text{ mmol l}^{-1} \text{ Na}^+$ - azide to avoid ammonia production from remaining microorganisms (Downie et al., 1979). After centrifugation (5000 g, 5 min, 4 °C) the ammonia concentration of the supernatant was determined (see below). A slight error towards higher values in total body ammonia concentration cannot be excluded due to possible proteolytic ammonia generation during the homogenization process.

Ammonia measurement

The concentration of total ammonia was measured in magnetically stirred samples using a gas-sensitive NH_3 electrode (Thermo Orion, Beverly, USA) connected to a pH meter. For the detailed method description refer to Weihrauch et al. (1998) (Martin et al., 2011; Weihrauch et al., 1998). Ammonia sensitivity of the electrode was high and amounted to $\pm 1.5 \text{ } \mu\text{mol l}^{-1}$ total ammonia in the concentration range of 50 to $200 \text{ } \mu\text{mol L}^{-1}$ and $\pm 1 \text{ } \mu\text{mol L}^{-1}$ total ammonia in the concentration range of 4 to $50 \text{ } \mu\text{mol l}^{-1}$. All standard curves were prepared using the corresponding experimental solutions.

Immunohistochemistry and Western blotting

Immunostaining was carried out essentially as described in Sánchez Alvarado and Newmark (Sanchez Alvarado and Newmark, 1999). In brief, whole animals were first treated with 2% HCl in H_2O for 5 min and fixed in Carnoy's fixative for 2 hours. After 1 hour in 100% methanol they were bleached with a cold lamp in 6% H_2O_2 /methanol for 16 to 20 hours at room temperature without shaking. Rehydration was done by a series of methanol/ PBSTx (phosphate buffered saline supplemented with 0.3% Triton x-100) washes (75%, 50%, 25%) for 10 min each at room temperature. After two washes in

100% PBSTx animals were blocked for 2 hours in 1% Rotiblock (Carl Roth GmbH, Karlsruhe, Germany) /PBSTx (blocking buffer) at room temperature. Subsequently, animals were incubated with primary antibodies (V-ATPase subunit B specific, raised in guinea pig against *Manduca sexta* antigen, diluted 1:100 (Weng et al., 2003)) for 20 hours at 4° C in blocking buffer. The negative control was incubated in parallel in the same buffer without addition of antibodies. 8 washes in PBSTx (1hour each) were followed by 1 hour in blocking buffer with all steps performed at room temperature. The secondary antibody (Cy3-conjugated anti guinea pig, Jackson ImmunoResearch, Newmarket, Suffolk, UK) was diluted 1:200 in blocking buffer and positive and negative samples were incubated for 14-16 hours at 4° C. Finally animals were washed for 3-4 hours in PBSTx at room temperature.

For cryosections (10 µm), stained specimens were subjected to an increasing sucrose gradient (10%, 20%, 30% in PBS) prior to embedding them in Tissue Freezing Medium (Jung, Germany). Freezing was conducted in isopentane cooled in liquid nitrogen. Subsequent to sectioning (Leica CM1900 cryomicrotome) frozen tissues were transferred to glass slides (superfrost, Microm international, Walldorf, Germany), fixed by short term warming (10 s, 50° C), washed 3 times (PBS, 5 min each) and embedded in VectaShield (Vector Laboratories, Burlingame, CA, USA). Sections were visualized using either a stereomicroscope (Leica MZ16 FA) or a confocal laser scanning microscope (LSM 5 Pascal, Zeiss).

Western blotting was carried out essentially as previously described (Meyer et al., 2009). Briefly, animals were homogenized (glass-teflon homogenizer) in PBS containing protease inhibitor mix M (Serva, Heidelberg, Germany). Subsequently, Laemmli buffer

was added and samples were boiled at 99° C for 3 min. Protein samples (15µg/lane) were separated by SDS-PAGE and transferred to nitrocellulose membranes. The primary antibody (anti V-ATPase subunit B) was applied at a dilution of 1:1000 and visualized by anti-guinea pig alkaline phosphatase conjugated antibody (1:10.000, Sigma).

In-situ hybridization and riboprobe synthesis

Whole-mount *in situ* hybridization was carried out as previously described (Umesono et al., 1999) including a triethanolamine treatment as described in (Nogi and Levin, 2005). Proteinase K (20 µg/ml) treatment was performed for 8 min at 37° C. The DIG-labelled riboprobes were used at 0.2 ng/µl for hybridization, which was performed at 55° C for 60 hours. Primers used for synthesis of the probes for Rh-like protein were (5' → 3') atgattcaaccatggggtgca (forward) and ttaaacttttcatttcgat (reverse) resulting in an amplicon of 486 base pairs. Subsequently, the respective sequence was cloned into the pGEM-T easy vector (Promega, Madison, WI, USA) and sense- as well as antisense- riboprobes were synthesized with “DIG RNA labelling kit” according to the manufacturer’s instructions (Roche, Mannheim, Germany).

Quantitative Real-Time PCR

For total RNA isolation animals with a combined weight of approximately 0.1 gFW were homogenized in TRIZOL reagent (Invitrogen, Carlsbad, CA, USA) employing a polytron homogenizer that was pre-treated with RNase AWAY™ (Invitrogen, Carlsbad, CA, USA). Following DNase treatment (DNase 1, Invitrogen, Carlsbad, CA, USA), RNA was tested for purity by a high cycle PCR using the primer pari actin F1/actin R1 (Table

1) targeting cytoplasmic actin (Genbank accession nr.: EG415476). For cDNA synthesis 1 µg of DNA free total RNA (showing no PCR products) was reversely transcribed using oligo (dT) primers and *Thermoscript* reverse transcriptase (Invitrogen, Carlsbad, CA, USA).

The quality of cDNAs generated from all tissues was assessed by PCR employing the primer pair actin F1/actin R1. All PCR products were evaluated by gel-electrophoresis, ethidium bromide staining and UV visualization. Primers to be employed in quantitative PCR targeting the Rh-like protein, V-ATPase (subunit A) and Na⁺/K⁺-ATPase (α -subunit) were designed based on published sequences (GenBank accession nos.: EG404114, EG416580, EG346594) and showed a single band of the predicted size after PCR and gel-visualization (Table 1). Sequencing of the purified PCR products (QIAquick Gel Extraction Kit, Qiagen Inc, Mississauga, Ontario, Canada) confirmed correctness of the amplicon. For quantitative PCR (Miniopticon, Biorad, Mississauga, Ontario, Canada), standard curves were generated using a dilution series with quantities of 10⁻², 10⁻³, 10⁻⁴, 10⁻⁵, 10⁻⁶, 10⁻⁷ ng DNA of the respective purified PCR product of the target gene. A minimum R² value of 0.98 for the standard curve was required. Real-time PCR assays were performed employing SsoFast EvaGreen supermix (Biorad, Mississauga, Ontario, Canada) in a 15 µl assay. After 40 cycles the quality of all PCR products were evaluated by performing a melting curve analysis as well as gel electrophoresis and ethidium bromide / UV visualization.

Chemicals

Unless stated otherwise, all chemicals were purchased from Sigma-Aldrich (St. Louis, MO, USA).

Statistics

Values are reported as the mean +/- standard error (SEM). Statistical tests performed included Student's t-tests for comparing two means and one-way ANOVA for comparing more than two means. P-values ≤ 0.05 were considered statistically significant. The statistical method employed in each particular experiment is given in the respective figure legends.

Results

Ammonia Excretion and Feeding

Under control conditions *Schmidtea mediterranea* excreted $0.70 \pm 0.03 \mu\text{mol}^{-1} \text{gFW}^{-1} \text{h}^{-1}$ ammonia (n=48) and whole body ammonia concentration was $1.9 \pm 0.1 \mu\text{mol} \text{gFW}^{-1}$ (n=6) (data not shown). Feeding increased excretion rates significantly. One hour after feeding ammonia excretion rates increased ca. 4-fold and reached a maximum three hours after feeding. Ammonia excretion rates declined slightly over time, but remained ~3-fold above the unfed controls 16 hours after feeding (Figure 1). One hour after ammonia excretion rates reached their maximum, relative mRNA expression levels of the Rh-protein and the V-ATPase (subunit A) were determined. At this time relative mRNA expression levels of the Rh-protein (n ≥ 3) were elevated (P < 0.038, one-tailed T-test). There was also a small but significant increase in the mRNA expression level of the V-

ATPase (subunit A) (n=4; Figure 2). The internal control used in all mRNA expression experiments was actin, which showed no difference in absolute mRNA expression levels after *S. mediterranea* was subjected to different treatments (n≥4) including a 2 day exposure to varying pH regimes and elevated ammonia concentrations (data not shown).

Short-Term Exposure to High Environmental Ammonia (HEA)

As seen in figure 3, short term exposure to 100 and 200 $\mu\text{mol L}^{-1}$ NH_4Cl had no effect of the excretion rates following HEA exposure. Short term exposure to 0.5, 1, 5 and 10 mmol L^{-1} NH_4Cl caused an increase in the excretion rate in the hour following the exposure, which decreased rapidly in the second hour after the treatment to control levels for 0.5 and 1 mmol L^{-1} NH_4Cl exposures and to near control levels for 5 and 10 mmol L^{-1} NH_4Cl exposures. Control levels were reached in the third hour after 10 mmol L^{-1} HEA exposure.

Ammonia Excretion Mechanism

Ammonia excretion in *S. mediterranea* depended on the acidification of the apical unstirred boundary layer of the epidermis. In comparison to excretion rates recorded in unbuffered freshwater (control, pH=8.3), higher and lower values were found in media buffered to pH 5 and above pH 7, respectively. In media buffered to a pH of 5.5, 6.0 and 6.5 ammonia excretion rates did not differ from rates measured under control conditions. Figure 4 shows excretion rates as percent of the respective controls (n=6 for all treatments).

Inhibition of the V-type H⁺-ATPase (V-ATPase) by addition of 5 μmol L⁻¹ concanamycin C to the environmental solution, reduced the ammonia excretion rate by 49.2 ± 5.4% (n=6). A similar reduction in the excretion rate was found after blockage of apical cation-proton exchangers (NHE) and/or Na⁺ channels employing 10 mmol L⁻¹ amiloride hydrochloride hydrate (n=6) or inhibiting the Na⁺/K⁺-ATPase by 1 mmol L⁻¹ ouabain (n=4). Moreover, a concentration of 1 mmol L⁻¹ acetazolamide, an inhibitor of the carbonic anhydrase, reduced the ammonia excretion rate by 37.8 ± 2.4 % (n=6). Disrupting the microtubule network by 10 mmol L⁻¹ colchicine (n=6) had no significant effect on the excretion rate (Figure 5). Application of 2 mmol L⁻¹ amiloride hydrochloride hydrate had no effect on the excretion rate (n=6, data not shown).

A monitoring period of one week following each experiment revealed that none of the treatments caused any mortality (data not shown). The inhibitory effect of acetazolamide (1 mmol L⁻¹) on the ammonia excretion rate was counteracted by lowering the medium pH from 8.3 (control) to pH 5 (buffered with MES) (n=4) (Figure 6).

As shown in figure 7A, in *S. mediterranea* protein extracts (whole animals), the V-ATPase antiserum detected a dominant protein band with a molecular mass of approximately 56 kDa, which corresponds to the molecular masses already calculated for B-subunits from other invertebrate species (Merzendorfer et al., 1997; Weihrauch et al., 2001). The distinct detection of this band is considered as strong indication for the presence of a V-ATPase in this organism, with its subunit B being recognized rather specifically by the applied antiserum.

Immunohistochemical analyses of *S. mediterranea* cross sections using the same antiserum, detected the V-ATPase (subunit B) in the epidermis of the animal (Figure 7B,

c, d, f, g) with an apparent accumulation in rod-shaped structures, presumably rhabdites (Figure 7B, f, g, arrows).

To analyze the expression pattern of the Rh-like ammonia transporter (GenBank accession #: DN307511) and to relate this pattern to V-ATPase expression, we generated riboprobes specific to the corresponding mRNA and used them for *in-situ* hybridizations. As depicted in figure 8, mRNA coding for the Rh-like protein was detected predominately in the epidermis. In control animals incubated with sense probes no staining was visible.

The Effect of Environmental pH

A two 2 day exposure to strongly buffered media adjusted to a pH of 8.5 caused a nearly 2-fold increase of the whole body ammonia concentration from $1.95 \pm 0.5 \mu\text{mol gFW}^{-1}$ (n=4) to $3.58 \pm 0.4 \mu\text{mol gFW}^{-1}$ (n=6), whereas exposure to media buffered to pH 5.5 (n=4) and pH 7 (n=5) caused a slight but significant decrease (Figure 9). In all applied external pH regimes (non-buffered freshwater (n=6); pH 5.5 (n=4); pH 7 (n=4) and pH 8.5 (n=6)), the body pH remained unaltered at 7.18 ± 0.06 (data not shown).

The relative mRNA expression levels for both the Rh-protein and the A subunit of the V-ATPase were correlated to medium pH (n \geq 4). Compared to controls (non-buffered media, pH 8.3) the low pH and high pH buffered media caused an up- and down-regulation of the Rh-protein, respectively, whereas a similar expression level was measured in animals exposed for two days to pH 7. Relative expression levels of the V-ATPase (subunit A) in animals exposed to pH 5.5 and 7 were up-regulated when

compared to controls, whereas in animals exposed to pH 8.5 the V-ATPase showed a trend towards down-regulation (Figure 10).

Long Term Exposure to High Environmental Ammonia (HEA)

Long term exposure to 5 and 10 mmol L⁻¹ NH₄Cl was lethal to *S. mediterranea*, causing death after 48 and 24 hours, respectively (n=6). Exposure of up to 1 mmol L⁻¹ NH₄Cl was tolerated by *S. mediterranea* for an extended time period of at least 1 week. After 48 hours of exposure to 0.1, 0.2, 0.5, and 1 mmol L⁻¹ NH₄Cl, body ammonia concentrations increased with increasing environmental ammonia concentrations (n=5) (Figure 11).

HEA also led to an increase in mRNA expression levels of the Rh-protein (0.5, 1 mmol L⁻¹ NH₄Cl; n=4) and the Na⁺/K⁺-ATPase (α-subunit) (1 mmol L⁻¹ NH₄Cl; n=4), but had no effect on relative mRNA expression levels of the V-ATPase (subunit A) (n=4) (Figure 12).

Discussion

Ammonia excretion rates measured in *Schmidtea mediterranea* fell within the range measured for other freshwater organisms. As a comparison, excretion rates for rainbow trout (*Oncorhynchus mykiss*) and *Xenopus laevis* tadpoles amount to ca. 0.4 μmol⁻¹ gFW⁻¹ h⁻¹ and 0.64 μmol⁻¹ gFW⁻¹ h⁻¹, respectively (Wildling and Kerschbaum, 2007; Zimmer et al., 2010). Rates for developing zebrafish larvae (9 days post fertilization) are ca. 2 μmol⁻¹ gFW⁻¹ h⁻¹ (Braun et al., 2009).

Immediately after feeding, ammonia excretion rates roughly quadrupled when compared to controls (Figure 1), an increase in metabolic ammonia production similar to that observed in the green shore crab *Carcinus maenas* (Weihrauch, 1999a) but much higher than values in rainbow trout (Zimmer et al., 2010), where excretion rates increase not directly after food intake but after a delay of approximately 2 to 4 hours. Feeding also leads to subsequent increases in mRNA expression levels of branchial Rhcg2 and the V-ATPases (subunit B) in trout (Zimmer et al., 2010). In the flatworm, the degree of increase of mRNA expression levels of the Rh-protein and the V-ATPases (subunit A) was comparatively low. However, here it is important to note that *S. mediterranea* RNA was isolated from whole animals and not from a particular ammonia excreting tissue. Changes in expression levels of the Rh-protein and the V-ATPase may thus be greater in the epidermis or other potential ammonia transporting tissues after treatments such as feeding. For *S. mediterranea* it is assumed that an up-regulation of the Rh-protein and the V-ATPase would promote ammonia excretion, when elevated excretion rates are necessary to maintain body fluid ammonia levels in a tolerable range. Unfortunately, in this study direct measurements of pH and ammonia concentrations in the interstitial fluid were not possible, so we could not put these parameters into perspective with excretion rates and changes and gene expression levels.

For an indirect estimation of the interstitial fluid ammonia levels and the capacity to maintain these ammonia levels within the body fluids, animals were exposed to a variety of different environmental ammonia concentrations for short periods and post-exposure excretion rates were monitored (Figure 3). After exposure to 100 and 200 μmol

$\text{L}^{-1} \text{NH}_4\text{Cl}$, ammonia excretion rates did not differ from control rates, suggesting that during this short-term exposure no ammonia was accumulated within the body fluids and ammonia excretion continued uncompromised. Consequently, the animals either possess an active or secondary active ammonia excretion mechanism, which functions when interstitial fluid levels are equal or below $200 \mu\text{mol L}^{-1}$ as seen in the hemolymph of decapod crabs (Martin et al., 2011; Weihrauch, 1999b), or have higher basal ammonia levels in their interstitial fluids, so that an outwardly ammonia gradient is maintained to grant excretion. In freshwater organisms hemolymph/blood ammonia concentrations between ca. 100 and $500 \mu\text{mol L}^{-1}$ are very common. For instance, in the hemolymph of the freshwater crayfish *Cherax destructor* (Fellows and Hird, 1979) and freshwater acclimated Chinese mitten crab *Eriocheir sinensis* (Weihrauch, 1999b) values of ca. 100 and $116 \mu\text{mol L}^{-1}$ were measured. In freshwater trout (Zimmer et al., 2010), the mudpuppy *Necturus maculosus*, and the fully aquatic African clawed frog *Xenopus laevis* (Wood et al., 1989) blood ammonia concentrations of ca. 550, 150 and $116 \mu\text{mol L}^{-1}$ were detected, respectively. A one hour exposure to $\geq 500 \mu\text{mol L}^{-1} \text{NH}_4\text{Cl}$ led to elevated post-exposure ammonia excretion rates, suggesting accumulation of ammonia within the body fluids during the treatment. It thus appears that ammonia excretion cannot counterbalance passive ammonia influxes at this level (Figure 11).

Ammonia excretion mechanism

The ammonia excretion rate in *S. mediterranea* was highly influenced by the ambient pH (Figure 4), suggesting an ammonia excretion mechanism based on ammonia trapping across the exposed body surface. Our data showed similar excretion rates in

non-buffered water (pH 8.3) and in media strongly buffered to a pH between 5.5 and 6.5, indicating that the animal itself acidifies the unstirred boundary layer to that range of pH to promote ammonia excretion. This was also evident in a greatly reduced excretion rate when the environmental media was buffered to pH 8 and pH 8.5, respectively. Our attempts to measure the acidification and ammonia excretion on the body surface directly by employing the SIET-technique (Donini and O'Donnell, 2005) failed due to the mucous layer that is excreted by the epidermis. Nevertheless, this mucous layer provides a microenvironment that most likely retains a low pH generated by the epidermis. The effects of inhibitors (Figure 5) are also consistent with acidification of the apical unstirred boundary layer by the epidermis. Inhibitory effects of concanamycin C, amiloride and acetazolamide provide evidence of the involvement of a V-ATPase and a cation/proton exchanger in this process. Both transporters utilizing protons provided by the activity of an intracellular carbonic anhydrase, a mechanism also suggested to function in the branchial pavement cells of freshwater fish (Nawata et al., 2007; Nawata and Wood, 2008; Nawata and Wood, 2009; Nawata et al., 2010b; Weihrauch et al., 2009). Participation of an apically localized NHE, *nhe3b*, in ammonia excretion has most convincingly been shown in flux studies employing inhibitor experiments and *nhe3b* knock-down experiments in zebrafish larvae (Shih et al., 2012). The importance of an apical H^+ -gradient in ammonia excretion is also evident by our data showing that even when acidification of the apical unstirred boundary layer by the V-ATPase and/or possibly an NHE is compromised due to the reduction of cytoplasmatic proton availability after inhibition of the carbonic anhydrase, an applied low apical pH enhanced the ammonia excretion rate to values well above control levels (Figure 6). Although

amiloride employed at higher concentrations blocks both NHEs and Na⁺-channels (Kleyman and Cragoe, 1988) which might be present in the apical membrane of the epidermal epithelium, 2 mmol L⁻¹ amiloride had no effect on ammonia excretion rates. This concentration is at least 3 orders of magnitudes higher than the IC₅₀ reported for Na⁺ channels (Kleyman and Cragoe, 1988), so an indirect inhibition of ammonia excretion due to a shift in membrane potential caused by a putative blockage of an apical Na⁺ channel seems unlikely.

Although an NHE8-like cation/proton exchanger has been cloned in *S. mediterranea* (GenBank accession #: EG354491) and blockage of the ammonia excretion rate by high doses of amiloride does suggest the participation of an apical NHE, there is to date no proof for the presence of such a transporter in the apical membrane of the hypodermis. There is an open debate whether an electroneutral Na⁺/H⁺ exchanger, which is driven only by the prevailing cation concentrations but not the electrical potential across the apical membrane, could function in freshwater environments, due the potential threat of Na⁺ loss (Orlowski and Grinstein, 2004; Parks et al., 2008). On the other hand, as mentioned above, there is recent evidence for the participation of an apically localized nhe3b in ammonia excretion in zebrafish larvae (Shih et al., 2012; Yan et al., 2007) and the presence of NHE2 and NHE3 in branchial Na⁺/K⁺-ATPase-positive PNA⁺ MRCs in rainbow trout (Ivanis et al., 2008). Moreover, there are precedents for electrogenic sodium:proton exchangers (*i.e.* 2Na⁺: 1H⁺) in invertebrates (Ahearn et al., 2001) which are inhibited by amiloride and which would allow the influx of Na⁺ to be driven in part by the transmembrane potential difference established by the electrogenic H⁺-ATPase.

Finally, it cannot be ruled out that amiloride's effects on the flatworms are mediated not through inhibition of an apical NHE and/or Na⁺-channel, but through blockade of a cation channel-like structure in the cuticle overlaying the hypodermis, as previously shown for the isolated cuticle of crustacean gills (Onken and Riestenpatt, 2002; Weihrauch et al., 2002). Clearly, more studies are necessary to evaluate the effects of amiloride on ammonia fluxes in *S. mediterranea*, including verification of the presence and the cellular localization of the NHE8-like or other NHE-like transporters in the hypodermis, as well as the characteristics of such transporters.

Employing an antibody raised against the subunit B of an invertebrate V-ATPase in cross sections of *S. mediterranea* confirmed abundance of the proton pump in the epidermis. The V-ATPase was particularly abundant in the rhabdites (Figure 7), consistent with their acidophilic characteristics (Reisinger and Klebetz, 1964; Stevenson and Beane, 2010). Although not shown explicitly in this study, an apical localization of the V-ATPase in the epidermal epithelium of *S. mediterranea* is plausible given widespread findings showing that proton pumps implicated in osmoregulatory NaCl uptake are localized to the apical surfaces in the skin and gills of freshwater organisms (Hwang, 2009; Klein et al., 1997; Lin et al., 2006; Onken and Putzenlechner, 1995; Patrick et al., 2006; Shih et al., 2008)

Apical exit of ammonia might be mediated by an Rh-like ammonia transporter which was highly expressed in the epidermis (Figure 8), although it cannot be excluded that the identified Rh-like ammonia transporter is also or exclusively localized in the basolateral membrane and mediates hemolymph to cell ammonia uptake. Involvement of this protein in ammonia excretion is also implicated by changes in its mRNA expression

level in response to changes of environmental pH, HEA and an internal ammonia load after feeding (Figures 2, 10, 12). In common with the teleost ammonia transporter Rhcg2, which is localized apically in the branchial pavement cells, the Rh-protein from *S. mediterranea* is up-regulated during long-term HEA. In contrast to Rhcg2, the basolateral ammonia transporter Rhbg is not influenced by HEA in freshwater fish (Nawata et al., 2007). Considering its similar response (up-regulation) to HEA (Nawata et al., 2007; Zimmer et al., 2010) and feeding (Zimmer et al., 2010) (Figures 2, 12), we suggest that the Rh-protein in *S. mediterranea* is also apically expressed and that it functions in a fashion comparable to that of the branchial Rhcg2 from freshwater fish. A more detailed analysis of this transporter, including functional expression analysis and cellular localization studies, is clearly needed to justify this suggestion. An analysis of the published partial amino acid sequence of *S. mediterranea* (GenBank accession #: DN307511) revealed a high degree of identity to Rh-proteins with confirmed ammonia transport capacities, including critical amino acids which are important for NH₃ conductance.

Basolateral entrance of extracellular ammonia into the cytoplasm of the ammonia excreting epithelia is possibly mediated by the Na⁺/K⁺-ATPase, as evident by the ca. 50% reduction of excretion after inhibition of the pump (Figure 5) and an mRNA up-regulation of its α -subunit after HEA (Figure 12). Comparatively high concentrations (1 mmol l⁻¹) of ouabain were required to obtain an inhibitory effect, since this pump is most likely inserted in the basolateral membrane and can thereby not be targeted directly. In both vertebrate and invertebrate systems the Na⁺/K⁺-ATPase accepts NH₄⁺ ions as a substrate, thereby facilitating the active transport of extracellular NH₄⁺ into the epithelial

cell (Furriel et al., 2004; Kurtz and Balaban, 1986; Mallery, 1983; Masui et al., 2002; Nawata et al., 2010a; Skou, 1960; Wall and Koger, 1994). Blockage of the Na⁺/K⁺-ATPase may also inhibit ammonia excretion indirectly due to a reduced “out-to-in” Na⁺-gradient and a consequent reduction in apical acidification via NHE if present.

An intracellular vesicular transport of NH₄⁺, as proposed for the branchial ammonia transport in the green shore crab *Carcinus maenas* (Weihrauch et al., 2002) or in the midgut of the tobacco hornworm *Manduca sexta* (Weihrauch, 2006) is unlikely, since application of a high concentration of the microtubule blocker colchicine showed no inhibitory effect on ammonia excretion by *S. mediterranea*. Responses of ammonia excretion rates measured after manipulations of the environmental media in short-term experiments suggests that a portion, if not the majority, of metabolic ammonia is indeed excreted via the body surface and not via the protonephridia since these short-term treatments would likely not have affected the internal excretory tissues. Moreover, the Rh-protein and V-ATPase, transporters involved in the ammonia excretory process were found in high abundance in the epidermis (Figures 7, 8). A hypothetical working model of the ammonia excretion mechanism suggested in the epidermal epithelium is summarized in figure 13.

The effect of long term exposure to varying pH regimes

Long-term exposure to varying environmental pH regimes caused changes in whole body ammonia levels and mRNA expression levels of the Rh-protein and V-ATPase, but had no effect on whole body pH. A two day exposure to an environmental pH of 5.5 caused a slight decrease in body ammonia concentration likely due to the body-

to-environment ΔP_{NH_3} (~ 50 fold outwardly directed NH_3 gradient) at this pH regime that favours NH_3 excretion. The relatively high mRNA expression level of Rh-protein observed after the exposure would promote NH_3 excretion. Moreover, it has been suggested that Rh-proteins also promote the transport of CO_2 (Musa-Aziz et al., 2009; Perry et al., 2010; Soupene et al., 2004). One could therefore further speculate that this high abundance of the Rh-protein in the epidermis promotes excretion of metabolic CO_2 in planarians stressed by low pH. In parallel, expression of the V-ATPase (subunit A) is also elevated, possibly to counteract the inward proton gradient and to maintain pH homeostasis.

As observed in trout embryos (Sashaw et al., 2010), exposure to a high environmental pH caused an accumulation of body ammonia levels in *S. mediterranea* (Figure 9) likely due to a hampered ammonia excretion at these unfavourable conditions as seen in figure 4. The corresponding down-regulation of the Rh-protein in *S. mediterranea* may serve as a protective mechanism to reduce the entrance of environmental NH_3 or the exit of metabolic CO_2 , the latter in order to retain acid equivalents. In parallel to the Rh-protein, the V-ATPase, which is also found in high abundance in the epidermis (Figure 7), showed a trend towards down-regulation relative to expression levels in animals exposed to pH 5.5 and pH 7 (Figure 10), respectively. Such a down-regulation would reduce active H^+ -loss into a media that cannot be acidified due to its artificial high buffer capacity but also energy consumption.

The effect of long term exposure to HEA

The whole body ammonia concentrations in *S. mediaterranea* ($1.9 \pm 0.1 \mu\text{mol gFW}^{-1}$) were similar to values measured in the freshwater ribbon leech *Nephelopsis obscura*, (Weihrauch, unpublished), however well above of those reported for trout embryos (ca. $0.25 \mu\text{mol gFW}^{-1}$) (Sashaw et al., 2010). Tolerance to high body ammonia and the capability for an active or secondary active ammonia excretion mode might be attributable to the benthic life style of many freshwater planarians (Lombardo et al., 2011). Long term exposure even to low environmental ammonia concentrations ($100 \mu\text{mol L}^{-1} \text{NH}_4\text{Cl}$) caused an increase in body ammonia levels, suggesting that normal ammonia concentrations in the interstitial fluids are fairly low.

In *S. mediterranea* relative mRNA expression levels of the Rh-like protein were up-regulated after exposure to HEA (Figure 12), a phenomena also observed for the apical localized Rhcg2 in embryonic and adult trout (Nawata et al., 2007; Sashaw et al., 2010) and also for branchial Rh-protein expression of a marine decapod crab (Martin et al., 2011). However, in contrast to trout (Nawata et al., 2007; Sashaw et al., 2010) and marine *Metacarcinus magister* crabs (Martin et al., 2011), the V-ATPase was not up-regulated after a two day HEA exposure, a puzzling finding since this pump, as discussed above, is most likely a key player in the ammonia excretion mechanism in *S. mediterranea*. A detailed analysis of the influence of HEA exposure on epidermal gene expression may provide further insight into the role this pump holds in ammonia excretion. The observed up-regulation of the Na^+/K^+ -ATPase after HEA exposure,

implies that this pump plays a significant role in ammonia homeostasis under challenging conditions.

Conclusions

This study provides the first comprehensive investigation of ammonia excretion mechanisms in a freshwater invertebrate species. Our findings suggest that the machinery that is involved in epidermal ammonia excretion in a planarian species is very similar to the excretion mechanism proposed to be functioning in the gills of freshwater fish. This mode of excretion may be quite common and may have evolved fairly early, prior to the appearance of vertebrates. *S. mediterranea* is amenable to a wide range of molecular techniques and will be of future use in determining the mechanisms of ammonia excretion at the molecular level.

Acknowledgements

We thank Dr, Helmut Wieczorek for providing the anti V-ATPase subunit B antiserum. The authors would like to thank the reviewers for their constructive comments in the review of this manuscript. This work was supported by NSERC Canada Discovery Grants to D.W. and M.J.O. and by the German Research Foundation to H.M. (SFB944).

Literature

Ahearn, G. A., Mandal, P. K. and Mandal, A. (2001). Biology of the $2\text{Na}^+/1\text{H}^+$ antiporter in invertebrates. *J Exp Zool* **289**, 232-44.

Blaesse, A. K., Broehan, G., Meyer, H., Merzendorfer, H. and Weihrauch, D. (2010). Ammonia uptake in *Manduca sexta* midgut is mediated by an amiloride sensitive

cation/proton exchanger: Transport studies and mRNA expression analysis of NHE7, 9, NHE8, and V-ATPase (subunit D). *Comp Biochem Physiol A Mol Integr Physiol* **157**, 364-76.

Braun, M. H., Steele, S. L., Ekker, M. and Perry, S. F. (2009). Nitrogen excretion in developing zebrafish (*Danio rerio*): a role for Rh proteins and urea transporters. *Am J Physiol Renal Physiol* **296**, F994-F1005.

Butterworth, R. F. (2002). Pathophysiology of hepatic encephalopathy: a new look at ammonia. *Metab Brain Dis* **17**, 221-7.

Cameron, J. N. and Heisler, N. (1983). Studies of ammonia in the rainbow trout: Physicochemical parameters, acid-base behaviour and respiratory clearance. *J Exp Biol* **105**, 107-125.

Chan, H., Hazell, A. S., Desjardins, P. and Butterworth, R. F. (2000). Effects of ammonia on glutamate transporter (GLAST) protein and mRNA in cultured rat cortical astrocytes. *Neurochem Int* **37**, 243-8.

Chintapalli, V. R., Wang, J. and Dow, J. A. (2007). Using FlyAtlas to identify better *Drosophila melanogaster* models of human disease. *Nat Genet* **39**, 715-20.

Civan, M. M., Rubenstein, D., Mauro, T. and O'Brien, T. G. (1985). Effects of tumor promoters on sodium ion transport across frog skin. *Am J Physiol* **248**, C457-65.

Cragg, M. M., Balinsky, J. B. and Baldwin, E. (1961). A comparative study of nitrogen excretion in some amphibia and reptiles. *Com Biochem Physiol* **3**, 227-235.

Donini, A. and O'Donnell, M. J. (2005). Analysis of Na⁺, Cl⁻, K⁺, H⁺ and NH₄⁺ concentration gradients adjacent to the surface of anal papillae of the mosquito *Aedes aegypti*: application of self-referencing ion-selective microelectrodes. *J Exp Biol* **208**, 603-10.

Downie, J. A., Gibson, F. and Cox, G. B. (1979). Membrane adenosine triphosphatases of prokaryotic cells. *Annu Rev Biochem* **48**, 103-31.

Fanelli, G. M. and Goldstein, L. (1964). Ammonia excretion in the neotenus newt, *Necturus maculosus* (Rafinesque) *Com Biochem Physiol* **13**, 193-204.

Fellows, F. C. I. and Hird, F. J. R. (1979). Nitrogen metabolism and excretion in the freshwater crayfish *Cherax destructor*. *Com Biochem Physiol* **64B**, 235-238.

Furriel, R. P., Masui, D. C., McNamara, J. C. and Leone, F. A. (2004). Modulation of gill Na⁺,K⁺-ATPase activity by ammonium ions: Putative coupling of nitrogen excretion and ion uptake in the freshwater shrimp *Macrobrachium olfersii*. *J Exp Zool A Comp Exp Biol* **301**, 63-74.

Hwang, P. P. (2009). Ion uptake and acid secretion in zebrafish (*Danio rerio*). *J Exp Biol* **212**, 1745-52.

Ip, Y. K. and Chew, S. F. (2010). Ammonia production, excretion, toxicity and defense in fish: a review. *frontiers in Physiology* **1** (134), 1-20.

Ivanis, G., Esbaugh, A. J. and Perry, S. F. (2008). Branchial expression and localization of SLC9A2 and SLC9A3 sodium/hydrogen exchangers and their possible role in acid-base regulation in freshwater rainbow trout (*Oncorhynchus mykiss*). *J Exp Biol* **211**, 2467-77.

Klein, U., Timme, M., Zeiske, W. and Ehrenfeld, J. (1997). The H⁺ pump in frog skin (*Rana esculenta*): identification and localization of a V-ATPase. *J Membr Biol* **157**, 117-26.

Kleyman, T. R. and Cragoe, E. J., Jr. (1988). Amiloride and its analogs as tools in the study of ion transport. *J Membr Biol* **105**, 1-21.

Knecht, K., Michalak, A., Rose, C., Rothstein, J. D. and Butterworth, R. F. (1997). Decreased glutamate transporter (GLT-1) expression in frontal cortex of rats with acute liver failure. *Neurosci Lett* **229**, 201-3.

Kurtz, I. and Balaban, R. S. (1986). Ammonium as a substrate for Na⁺-K⁺-ATPase in rabbit proximal tubules. *Am J Physiol* **250**, F497-502.

Lin, L. Y., Horng, J. L., Kunkel, J. G. and Hwang, P. P. (2006). Proton pump-rich cell secretes acid in skin of zebrafish larvae. *Am J Physiol Cell Physiol* **290**, C371-8.

Lombardo, P., Giustini, M., Miccoli, F. P. and Cicolani, B. (2011). Fine-scale differences in diel activity among nocturnal freshwater planarias (Platyhelminthes: Tricladida). *J Circadian Rhythms* **9**, 2.

Lucu, C., Devescovi, M. and Siebers, D. (1989). Do amiloride and ouabain affect ammonia fluxes in perfused *Carcinus* gill epithelia? *J Exp Zool* **249**, 1-5.

Mallery, C. H. (1983). A carrier enzyme basis for ammonium excretion in teleost gill. NH₄⁺-stimulated Na-dependent ATPase activity in *Opsanus beta*. *Comp Biochem Physiol A Comp Physiol* **74**, 889-97.

Marcaida, G., Felipo, V., Hermenegildo, C., Minana, M. D. and Grisolia, S. (1992). Acute ammonia toxicity is mediated by the NMDA type of glutamate receptors. *FEBS Lett* **296**, 67-8.

Marini, A. M., Matassi, G., Raynal, V., Andre, B., Cartron, J. P. and Cherif-Zahar, B. (2000). The human Rhesus-associated RhAG protein and a kidney homologue promote ammonium transport in yeast. *Nat Genet* **26**, 341-4.

Martin, M., Fehsenfeld, S., Sourial, M. M. and Weihrauch, D. (2011). Effects of high environmental ammonia on branchial ammonia excretion rates and tissue Rh-protein mRNA expression levels in seawater acclimated Dungeness crab *Metacarcinus magister*. *Comp Biochem Physiol A Mol Integr Physiol* **160**, 267-77.

Masui, D. C., Furriel, R. P., McNamara, J. C., Mantelatto, F. L. and Leone, F. A. (2002). Modulation by ammonium ions of gill microsomal (Na⁺,K⁺)-ATPase in the swimming crab *Callinectes danae*: a possible mechanism for regulation of ammonia excretion. *Comp Biochem Physiol C Toxicol Pharmacol* **132**, 471-82.

Merzendorfer, H., Graf, R., Huss, M., Harvey, W. R. and Wiczorek, H. (1997). Regulation of proton-translocating V-ATPases. *J Exp Biol* **200**, 225-35.

Meyer, H., Panz, M., Zmojdian, M., Jagla, K. and Paululat, A. (2009). Nephilysin 4, a novel endopeptidase from *Drosophila melanogaster*, displays distinct substrate specificities and exceptional solubility states. *J Exp Biol* **212**, 3673-83.

Musa-Aziz, R., Chen, L. M., Pelletier, M. F. and Boron, W. F. (2009). Relative CO₂/NH₃ selectivities of AQP1, AQP4, AQP5, AmtB, and RhAG. *Proc Natl Acad Sci U S A* **106**, 5406-11.

Nawata, C. M., Hirose, S., Nakada, T., Wood, C. M. and Kato, A. (2010a). Rh glycoprotein expression is modulated in pufferfish (*Takifugu rubripes*) during high environmental ammonia exposure. *J Exp Biol* **213**, 3150-60.

Nawata, C. M., Hung, C. C., Tsui, T. K., Wilson, J. M., Wright, P. A. and Wood, C. M. (2007). Ammonia excretion in rainbow trout (*Oncorhynchus mykiss*): evidence for Rh glycoprotein and H⁺-ATPase involvement. *Physiol Genomics* **31**, 463-74.

Nawata, C. M. and Wood, C. M. (2008). The effects of CO₂ and external buffering on ammonia excretion and Rhesus glycoprotein mRNA expression in rainbow trout. *J Exp Biol* **211**, 3226-36.

Nawata, C. M. and Wood, C. M. (2009). mRNA expression analysis of the physiological responses to ammonia infusion in rainbow trout. *J Comp Physiol B* **179**, 799-810.

Nawata, C. M., Wood, C. M. and O'Donnell, M. J. (2010b). Functional characterization of Rhesus glycoproteins from an ammoniotelic teleost, the rainbow trout, using oocyte expression and SIET analysis. *J Exp Biol* **213**, 1049-59.

Nogi, T. and Levin, M. (2005). Characterization of innexin gene expression and functional roles of gap-junctional communication in planarian regeneration. *Dev Biol* **287**, 314-35.

Norenberg, M. D., Huo, Z., Neary, J. T. and Roig-Cantesano, A. (1997). The glial glutamate transporter in hyperammonemia and hepatic encephalopathy: relation to energy metabolism and glutamatergic neurotransmission. *Glia* **21**, 124-33.

Onken, H. and McNamara, J. C. (2002). Hyperosmoregulation in the red freshwater crab *Dilocarcinus pagei* (Brachyura, Trichodactylidae): structural and functional asymmetries of the posterior gills. *J Exp Biol* **205**, 167-75.

Onken, H. and Putzenlechner, M. (1995). A V-ATPase drives active, electrogenic and Na⁺-independent Cl⁻ absorption across the gills of *Eriocheir sinensis*. *J Exp Biol* **198**, 767-74.

Onken, H. and Riestenpatt, S. (2002). Ion transport across posterior gills of hyperosmoregulating shore crabs (*Carcinus maenas*): amiloride blocks the cuticular Na⁽⁺⁾ conductance and induces current-noise. *J Exp Biol* **205**, 523-31.

Orlowski, J. and Grinstein, S. (2004). Diversity of the mammalian sodium/proton exchanger SLC9 gene family. *Pflugers Arch* **447**, 549-65.

Parks, S. K., Tresguerres, M. and Goss, G. G. (2008). Theoretical considerations underlying Na⁽⁺⁾ uptake mechanisms in freshwater fishes. *Comp Biochem Physiol C Toxicol Pharmacol* **148**, 411-8.

Patrick, M. L., Aimanova, K., Sanders, H. R. and Gill, S. S. (2006). P-type Na⁺/K⁺-ATPase and V-type H⁺-ATPase expression patterns in the osmoregulatory organs of larval and adult mosquito *Aedes aegypti*. *J Exp Biol* **209**, 4638-51.

Perry, S. F., Braun, M. H., Noland, M., Dawdy, J. and Walsh, P. J. (2010). Do zebrafish Rh proteins act as dual ammonia-CO₂ channels? *J Exp Zool A Ecol Genet Physiol* **313**, 618-21.

Potts, W. T. (1965). Ammonia Excretion in Octopus Dofleini. *Comp Biochem Physiol* **14**, 339-55.

Reisinger, E. and Klebetz, S. (1964). Fine structure and discharge mechanism of rhabdites. *Zeitschrift für Wissenschaftliche Mikroskopie und für Mikroskopische Technik* **65**, 472-508.

Rompolas, P., Patel-King, R. S. and King, S. M. (2009). Schmidtea mediterranea: a model system for analysis of motile cilia. *Methods Cell Biol* **93**, 81-98.

Sanchez Alvarado, A. and Newmark, P. A. (1999). Double-stranded RNA specifically disrupts gene expression during planarian regeneration. *Proc Natl Acad Sci U S A* **96**, 5049-54.

Sanchez Alvarado, A. and Tsonis, P. A. (2006). Bridging the regeneration gap: genetic insights from diverse animal models. *Nat Rev Genet* **7**, 873-84.

Sashaw, J., Nawata, M., Thompson, S., Wood, C. M. and Wright, P. A. (2010). Rhesus glycoprotein and urea transporter genes in rainbow trout embryos are upregulated in response to alkaline water (pH 9.7) but not elevated water ammonia. *Aquat Toxicol* **96**, 308-13.

Shih, T. H., Horng, J. L., Hwang, P. P. and Lin, L. Y. (2008). Ammonia excretion by the skin of zebrafish (*Danio rerio*) larvae. *Am J Physiol Cell Physiol* **295**, C1625-32.

Shih, T. H., Horng, J. L., Liu, S. T., Hwang, P. P. and Lin, L. Y. (2012). Rhcg1 and NHE3b are involved in ammonium-dependent sodium uptake by zebrafish larvae acclimated to low-sodium water. *Am J Physiol Regul Integr Comp Physiol* **302**, R84-93.

Skou, J. C. (1960). Further investigations on a $Mg^{++} + Na^{+}$ -activated adenosinetriphosphatase, possibly related to the active, linked transport of Na^{+} and K^{+} across the nerve membrane. *Biochim Biophys Acta* **42**, 6-23.

Soupe, E., Inwood, W. and Kustu, S. (2004). Lack of the Rhesus protein Rh1 impairs growth of the green alga *Chlamydomonas reinhardtii* at high CO_2 . *Proc Natl Acad Sci U S A* **101**, 7787-92.

Stevenson, C. G. and Beane, W. S. (2010). A low percent ethanol method for immobilizing planarians. *PLoS One* **5**.

Umesono, Y., Watanabe, K. and Agata, K. (1999). Distinct structural domains in the planarian brain defined by the expression of evolutionarily conserved homeobox genes. *Dev Genes Evol* **209**, 31-9.

Wall, S. M. and Koger, L. M. (1994). NH_4^{+} transport mediated by Na^{+} - K^{+} -ATPase in rat inner medullary collecting duct. *Am J Physiol* **267**, F660-70.

Weber, W. M., Liebold, K. M. and Clauss, W. (1995). Amiloride-sensitive Na^{+} conductance in native *Xenopus* oocytes. *Biochim Biophys Acta* **1239**, 201-6.

Weihrauch, D. (1999a). Zur Stickstoff-Exkretion aquatischer Brachyuren: *Carcinus maenas* (Linnaeus 1758, Decapoda, Portunidae), *Cancer pagurus* Linnaeus 1758 (Decapoda, Cancridae) und *Eriocheir sinensis* H. Milne Edwards 1853 (Decapoda, Grapsidae) Berlin: VWF Verlag fuer Wissenschaft und Forschung, GmbH.

Weihrauch, D. (2006). Active ammonia absorption in the midgut of the Tobacco hornworm *Manduca sexta* L.: Transport studies and mRNA expression analysis of a Rhesus-like ammonia transporter. *Insect Biochem Mol Biol* **36**, 808-21.

Weihrauch, D., Becker, W., Postel, U., Riestenpatt, S. and Siebers, D. (1998). Active excretion of ammonia across the gills of the shore crab *Carcinus maenas* and its relation to osmoregulatory ion uptake. *J Comp Physiol [B]* **168**, 364-376.

Weihrauch, D., Becker, W., Postel, U., Luck-Kopp, S. and Siebers, D. (1999b). Potential of active excretion of ammonia in three different haline species of crabs. *J Comp Physiol B* **169**, 25-37.

Weihrauch, D., McNamara, J. C., Towle, D. W. and Onken, H. (2004a). Ion-motive ATPases and active, transbranchial $NaCl$ uptake in the red freshwater crab, *Dilocarcinus pagei* (Decapoda, Trichodactylidae). *J Exp Biol* **207**, 4623-31.

Weihrauch, D., Morris, S. and Towle, D. W. (2004b). Ammonia excretion in aquatic and terrestrial crabs. *J Exp Biol* **207**, 4491-504.

Weihrauch, D., Wilkie, M. P. and Walsh, P. J. (2009). Ammonia and urea transporters in gills of fish and aquatic crustaceans (vol 212, pg 1716, 2009). *Journal Of Experimental Biology* **212**, 2879-2879.

Weihrauch, D., Ziegler, A., Siebers, D. and Towle, D. W. (2001). Molecular characterization of V-type H(+)-ATPase (B-subunit) in gills of euryhaline crabs and its physiological role in osmoregulatory ion uptake. *J Exp Biol* **204**, 25-37.

Weihrauch, D., Ziegler, A., Siebers, D. and Towle, D. W. (2002). Active ammonia excretion across the gills of the green shore crab *Carcinus maenas*: participation of Na(+)/K(+)-ATPase, V-type H(+)-ATPase and functional microtubules. *J Exp Biol* **205**, 2765-75.

Weng, X. H., Huss, M., Wiczorek, H. and Beyenbach, K. W. (2003). The V-type H(+)-ATPase in Malpighian tubules of *Aedes aegypti*: localization and activity. *J Exp Biol* **206**, 2211-9.

Wildling, S. and Kerschbaum, H. H. (2007). Nitric oxide decreases ammonium release in tadpoles of the clawed frog, *Xenopus laevis*, Daudin. *J Comp Physiol B* **177**, 401-11.

Wilson, R., Wright, P., Munger, S. and Wood, C. (1994). Ammonia excretion from freshwater Rainbow trout (*Oncorhynchus mykiss*) and the importance of gill boundary layer acidification: Lack of evidence for Na⁺/NH₄⁺ exchange. *J Exp Biol* **191**, 37-58.

Wood, C. M., Munger, R. S. and Toews, D. P. (1989). Ammonia, urea and H⁺ distribution and the evolution of ureotelism in amphibians. *J Exp Biol* **144**, 215-233.

Wright, P. A. (1995). Nitrogen excretion: three end products, many physiological roles. *J Exp Biol* **198**, 273-81.

Wright, P. A. and Wood, C. M. (2009). A new paradigm for ammonia excretion in aquatic animals: role of Rhesus (Rh) glycoproteins. *J Exp Biol* **212**, 2303-12.

Yan, J. J., Chou, M. Y., Kaneko, T. and Hwang, P. P. (2007). Gene expression of Na⁺/H⁺ exchanger in zebrafish H⁺ -ATPase-rich cells during acclimation to low-Na⁺ and acidic environments. *Am J Physiol Cell Physiol* **293**, C1814-23.

Zimmer, A. M., Nawata, C. M. and Wood, C. M. (2010). Physiological and molecular analysis of the interactive effects of feeding and high environmental ammonia on branchial ammonia excretion and Na(+) uptake in freshwater rainbow trout. *J Comp Physiol B*.

Table 1: Primers employed in real-time PCR targeting Rhesus-like ammonia transporter, V-type H⁺-ATPase (subunit A), Na⁺/K⁺-ATPase (α -subunit) and actin from *Schmidtea mediterranea*.

Primer	Nucleotide sequence (5' → 3')	Annealing Temp. (°C)	Product size (bp)
<i>Rh-protein</i>			
RhF2	GGTATGCCTGGTATCATGGG	60	285
RhR2	CGTCTCTTCTGAAACGGTCCA	60	
<i>H⁺-ATPase</i>			
HAT F1	ACCTTAGAAGTGGCCCGTTT	60	211
HAT R1	TGGTATCACCCATTGCTTCA	60	
<i>Na⁺/K⁺-ATPase</i>			
NaK F1	TCAGGAATGGGGATTTCAGAC	60	261
NaK R1	GGTAGCCACCACGTGAATCT	60	
<i>Actin</i>			
Actin F1	TTGGCCGGTAGAGATTTGAC	55	156
Actin R1	AGCTGCAGTTGCCATTCTT	55	

Figure legends

Figure 1: Ammonia excretion rates (means \pm SEM) of *S. mediterranea* before (control, Ctr) and after a feeding period of 1 hour (n=6). Significant differences are indicated by different letters. Data were analyzed employing a one-way Anova with repeated measures using a Tukey's pairwise comparison.

Figure 2: Relative mRNA expression levels (means \pm SEM) of the Rh-like protein (n \geq 3) and V-ATPase (subunit A) (n=4) in *S. mediterranea* before and 4 hours after feeding. The ratio of absolute expression levels of the target genes and actin is shown. The asterisk (*) indicates significant differences between treatment. Data were analyzed employing an one tailed student's t-test.

Figure 3: Ammonia excretion rates (means \pm SEM) of *S. mediterranea* before (control) and after short term exposure (1 hour) to different high environmental ammonia (HEA) concentrations (0.1, 0.2, 0.5, 1, 5 and 10 mmol L⁻¹ NH₄Cl) (n=6 for all treatments). Ammonia excretion rates of four consecutive hours after feeding are shown, the first hour after HEA exposure is indicated. Significant differences are indicated by different letters. Data were analyzed employing a one-way Anova with repeated measures using a Tukey's pair wise comparison.

Figure 4: Ammonia excretion of *S. mediterranea* in media adjusted and buffered to various pH regimes. The values represented indicate the percentage of the control (means \pm SEM). Control conditions = dechlorinated tap water (pH=8.3). Excretion rates are given in percent of controls (n=6 for all pH regimes). Significant differences to the control value are indicated by “*”. Data were analyzed statistically employing a paired student’s t-test (two-tailed) on the original excretion rate values.

Figure 5: Effects of different inhibitors on ammonia excretion rates (means \pm SEM) in *S. mediterranea*. Control values for each treatment were set to 100% (open bars), with values measured under the influence of the inhibitors are given as percent of the respective control (closed bars). The concentrations of the inhibitors (in brackets) were: concanamycin C (5 $\mu\text{mol L}^{-1}$, n=6); acetazolamide (1 mmol L^{-1} , n=6); amiloride (10 mmol L^{-1} , n=6); ouabain (1 mmol L^{-1} , n=4); colchicine (10 mmol L^{-1} , n=6). Significant differences from the control value are indicated by “*”. Data were analyzed employing a paired student’s t-test (two-tailed) on excretion rates prior to calculation of percentage values.

Figure 6: Effect of acetazolamide and low pH (pH 5.5, 10 mmol L^{-1} MES) on ammonia excretion rates (means \pm SEM) in *S. mediterranea*. Values are given as percentage of values measured without addition of any inhibitor (n=4). Data were analyzed on the non-transformed values employing a one-way Anova with repeated measures using a Tukey’s pair wise comparison.

Figure 7: Expression of V-ATPase subunit B in *Schmidtea mediterranea*. *A*, total protein extracts isolated from whole animals were probed with an antiserum raised against V-ATPase subunit B from *M. sexta*. A distinct band of approximately 56 kDa (calculated by migration distance), apparently V-ATPase subunit B, is detected, confirming expression of this subunit in *S. mediterranea*. *B*, in cross sections, the same antiserum detected a distinct signal in the epidermis of the animal which is mainly based on the staining of rod-shaped structures, presumably rhabdites (arrows). *a*, controls without application of primary antibody; *b*, *e*, brightfield; *a*, *c*, *f*, fluorescence; *d*, merge (*b*+*c*); *g*, merge (*e*+*f*). Magnifications are: *a*, *b*, *c*, *d* = 100x; *e*, *f* = 400x.

Figure 8: Expression of Rh-like protein in *Schmidtea mediterranea*. In whole mount preparations, application of antisense riboprobes specific to Rh-like protein mRNA resulted in a strong staining covering the complete animal (*A*). At higher magnifications the strongest signal intensity was apparent at the periphery of the animals, presumably in the epidermis (*A*′). Application of sense probes did not elicit any signal (*B*, *B*′). In cross sections, application of antisense riboprobes again resulted in a staining that resided mainly in the periphery of the animals, presumably epidermal cells (*C*, arrow), while sections incubated with sense probes did not show any staining (*D*, arrow). Magnifications are: *A*, *B*, 30x; *A*′, *B*′, 250x; *C*, *D*, 100x.

Figure 9: Whole body ammonia concentrations (means ± SEM) in *S. mediterranea* after 48 hours of exposure to control media (dechlorinated tap water, pH=8.3; n=4) and media

buffered to a pH of 5.5 (10 mmol L⁻¹ MES; n=4), 7 (10 mmol L⁻¹ HEPES, n=4) and 8.5 (10 mmol L⁻¹ TRIS, n=6), respectively. Significant differences are indicated by different letters. Data were analyzed employing a one-way Anova using a Tukey's pair wise comparison.

Figure 10: Relative mRNA expression levels (means \pm SEM) of the Rh-like protein (upper panel, n \geq 4) and V-ATPase (subunit A) (lower panel, n \geq 4) in *S. mediterranea* under control conditions and after a 48 hour exposure to media buffered to a pH of 5.5 (10 mmol L⁻¹ MES), 7 (10 mmol L⁻¹ HEPES) and 8.5 (10 mmol L⁻¹ TRIS), respectively. The ratio of absolute expression levels of the target genes and actin is shown. Significant differences are indicated by different letters. Data were analyzed employing a one-way Anova using a Tukey's pair wise comparison.

Figure 11: Body ammonia concentrations (means \pm SEM) in *S. mediterranea* after 48 hours exposure to control media (dechlorinated tap water, pH=8.3) and different high environmental ammonia concentrations (HEA; 0.1, 0.2, 0.5 and 1 mmol L⁻¹ NH₄Cl) (n=5 for all treatments). Significant differences are indicated by different letters. Data were analyzed employing a one-way Anova using a Tukey's pair wise comparison.

Figure 12: Relative mRNA expression levels (means \pm SEM) of the Rh-like protein, V-ATPase (subunit A) and Na⁺/K⁺-ATPase (α -subunit) in *S. mediterranea* under control conditions and after a 48 hour exposure to HEA (0.5 and 1 mmol L⁻¹ NH₄Cl; n=4 for all treatments). The ratio of absolute expression levels of the target genes and actin is shown.

Significant differences are indicated by different letters. Data were analyzed employing a one-way Anova using a Tukey's pair wise comparison.

Figure 13: Proposed hypothetical model of ammonia excretion across the epidermal epithelium in the freshwater planarian *Schmidtea mediterranea*. Hemolymph NH_4^+ is pumped across the basolateral membrane by the Na^+/K^+ -ATPase into the cytoplasm or enters as NH_3 via an Rh-like ammonia transporter. Protons generated by a cytoplasmic carbonic anhydrase are transported via an apical V-ATPase and possibly also via a cation/proton exchanger (NHE) across the apical membrane, acidifying the unstirred boundary layer to a pH of approximately 5.5-6.5. The low pH traps NH_3 as NH_4^+ as it passively diffuses into the unstirred boundary water along the maintained transcellular P_{NH_3} gradient. It is proposed that an identified Rh-like ammonia transporter mediates this apical NH_3 transport. Transport characteristics and basolateral versus apical localization of the planarian ammonia transporter (Rh-protein) are presently unknown (indicated by ?). The model assumes that paracellular NH_4^+ diffusion is negligible, given that in freshwater organisms epithelia facing the environment generally show a very low ion conductance to avoid passive effluxes along a steep osmotic gradient (Civan et al., 1985; Weber et al., 1995; Weihrauch, 1999b).

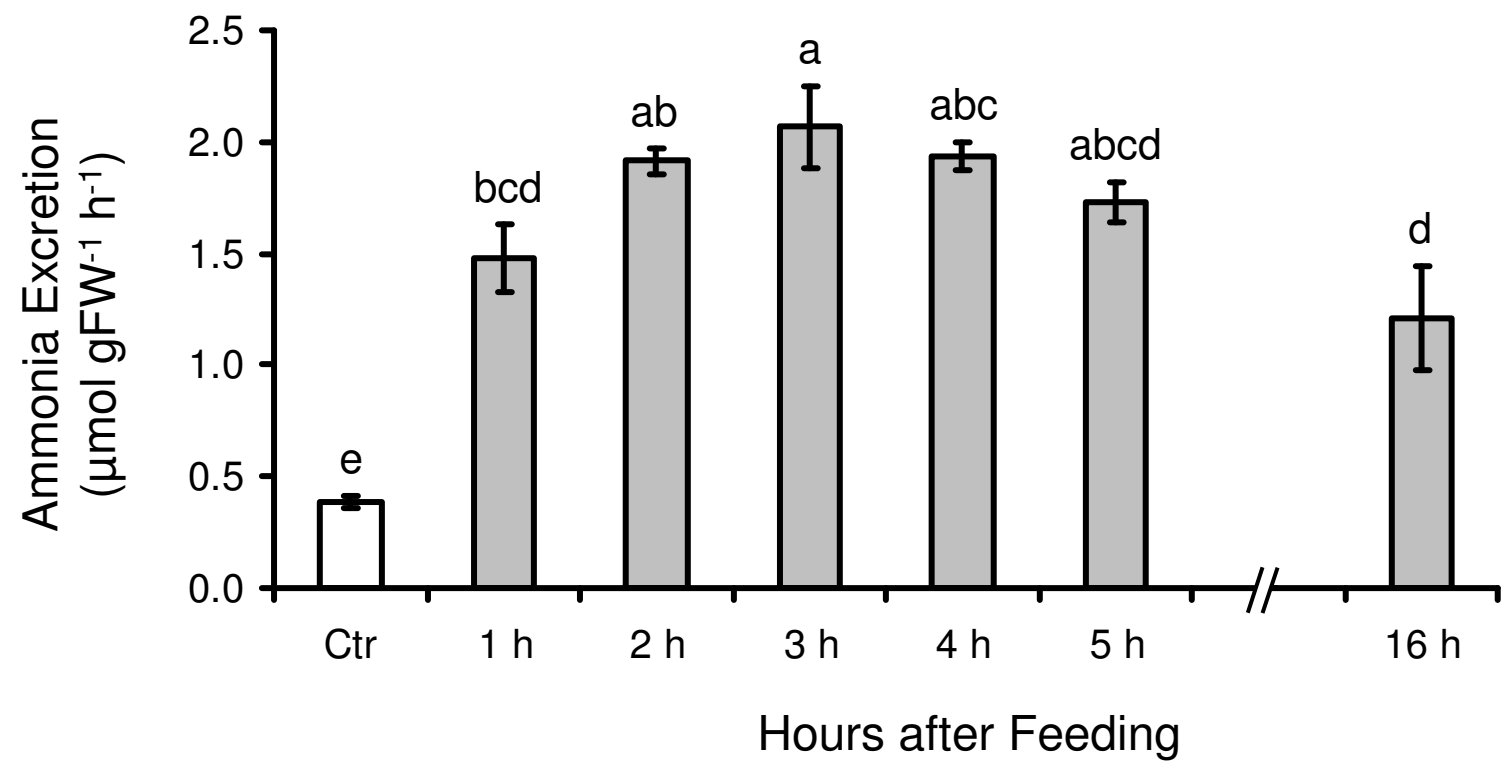


Figure 1

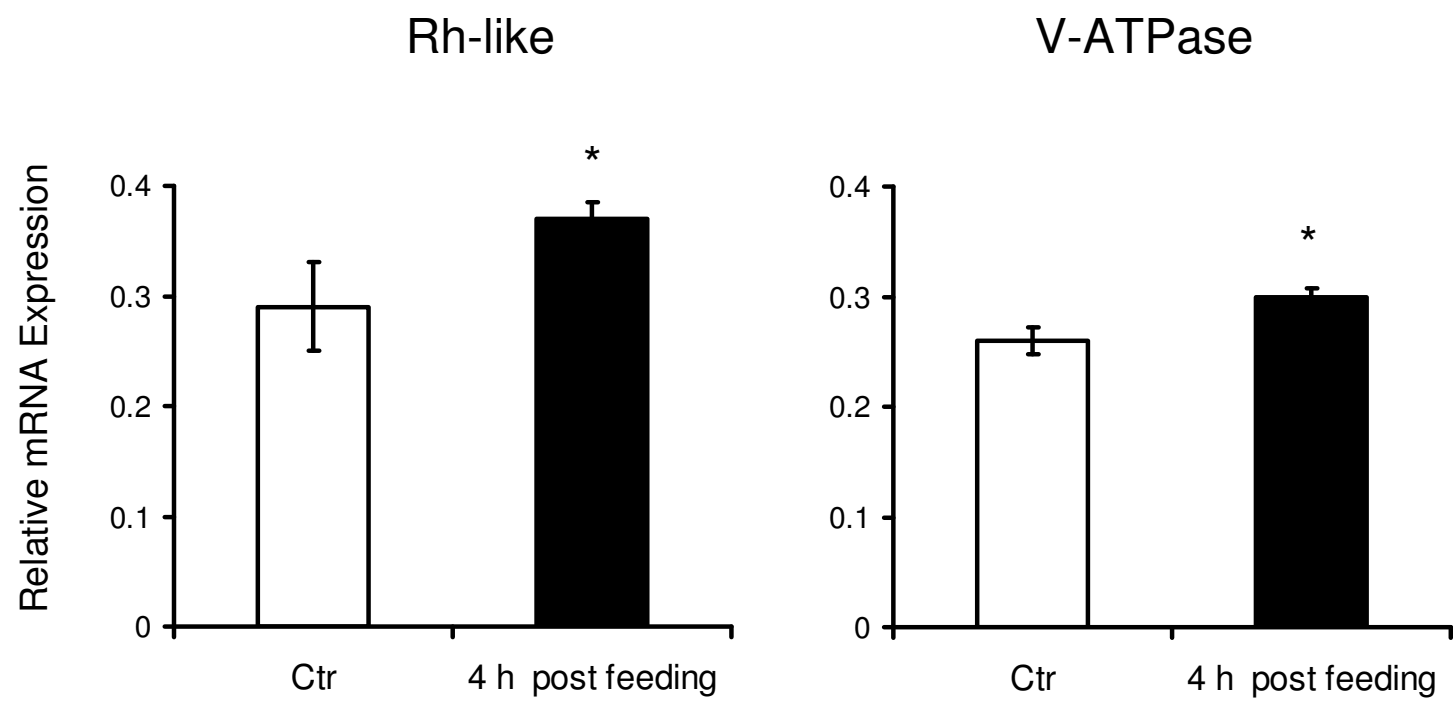


Figure 2

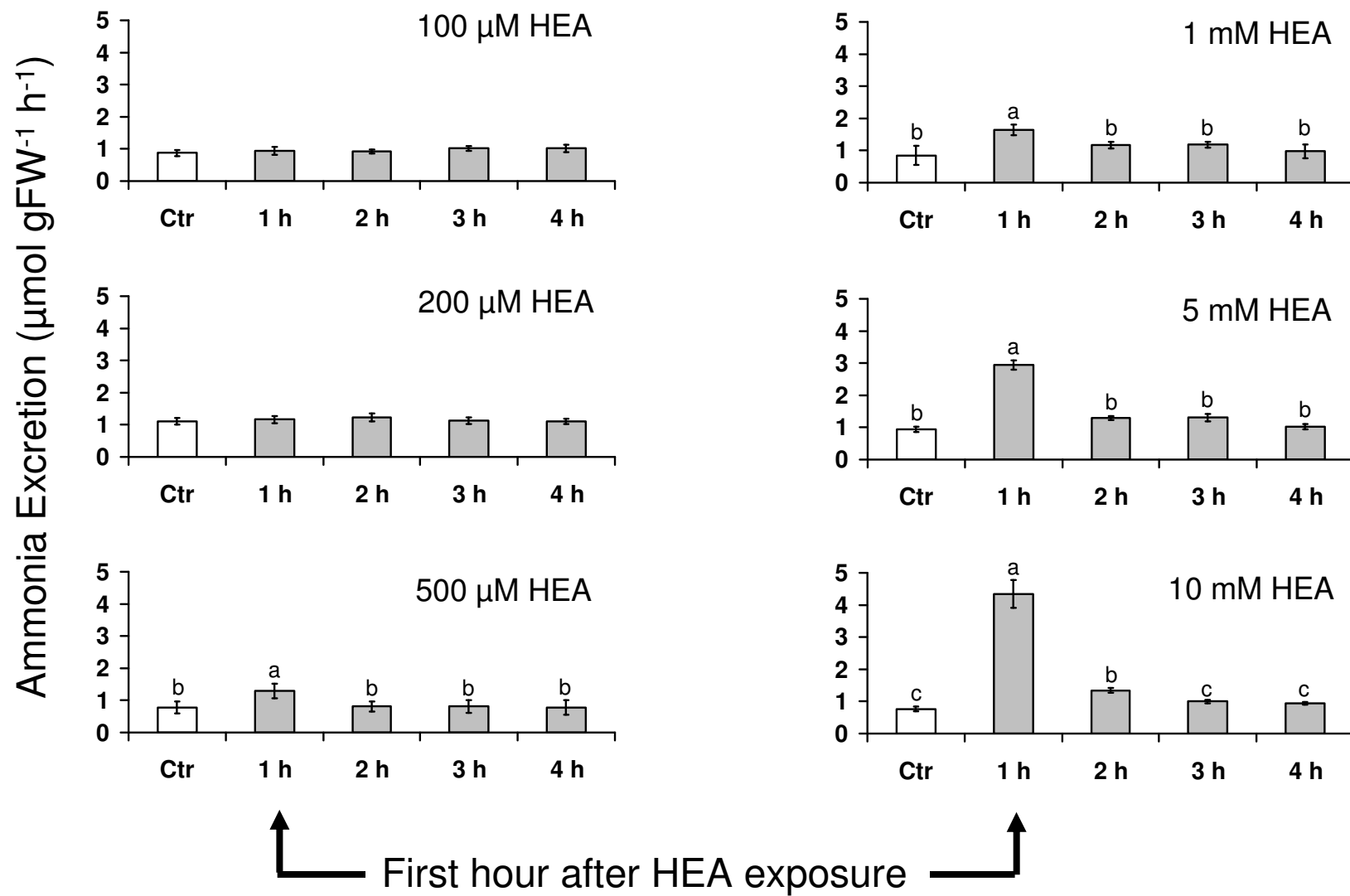


Figure 3

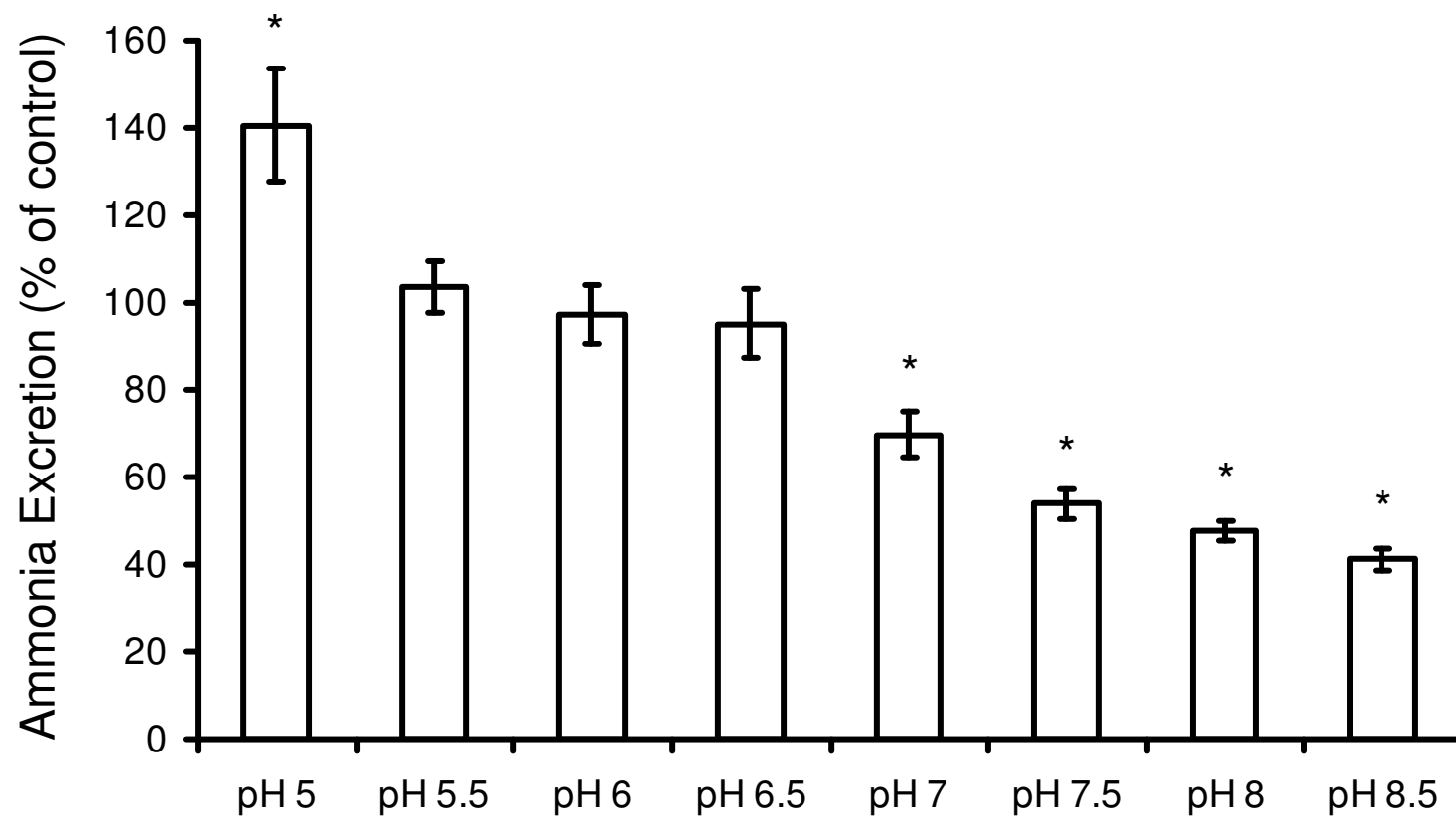


Figure 4

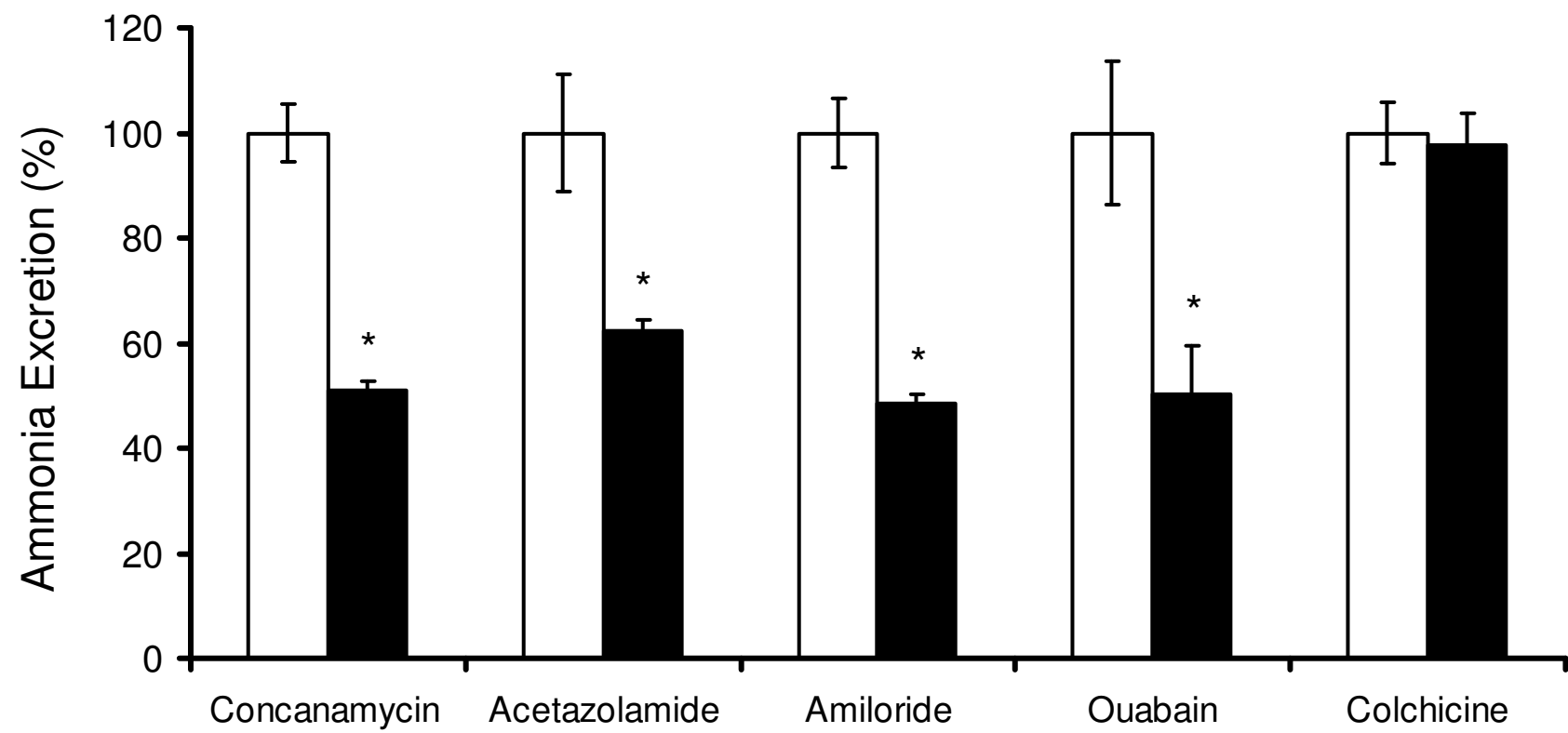


Figure 5

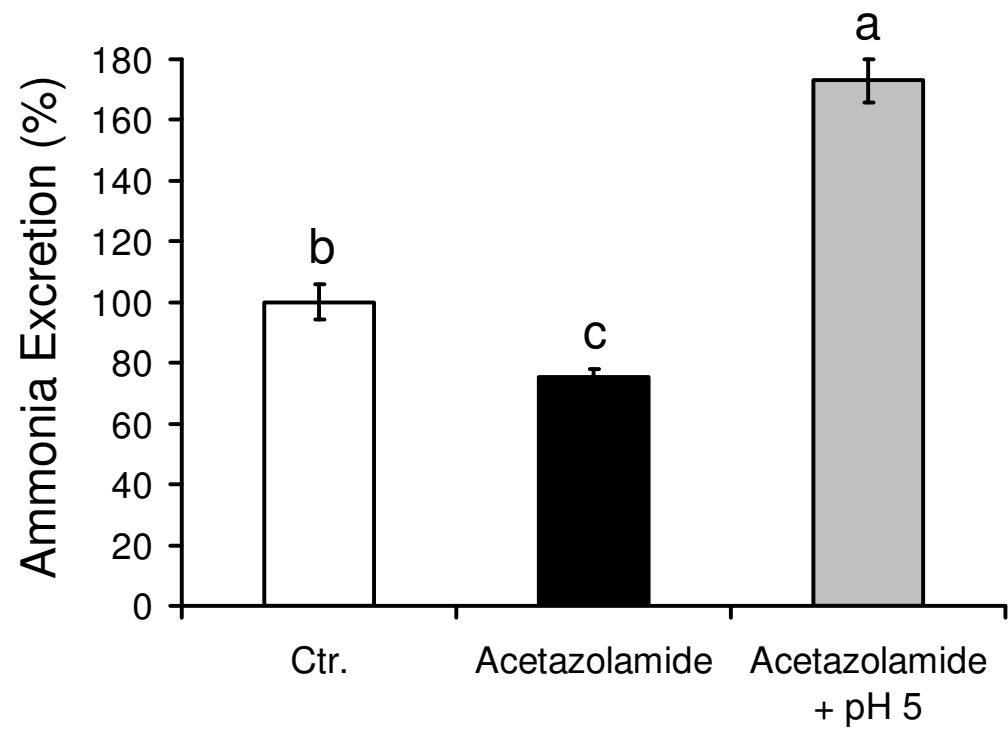
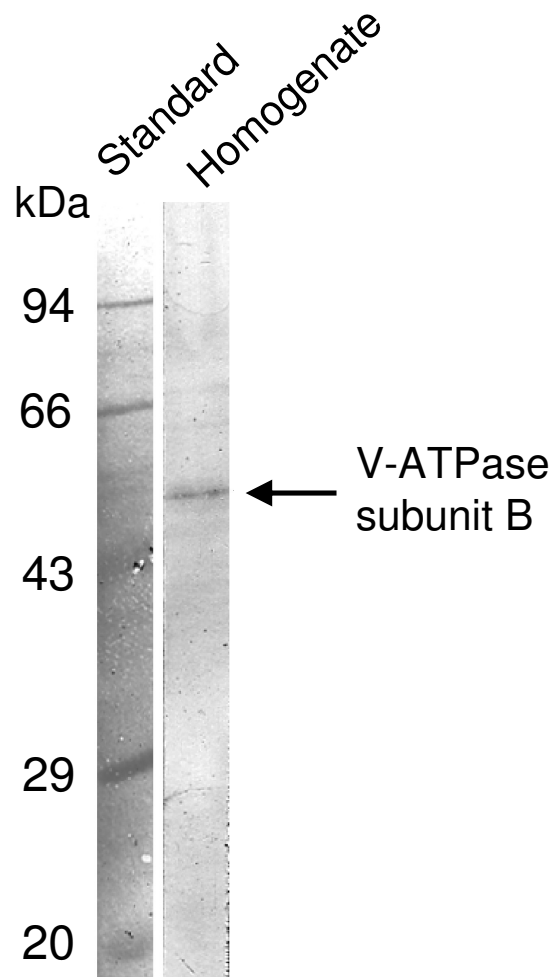


Figure 6

A



B

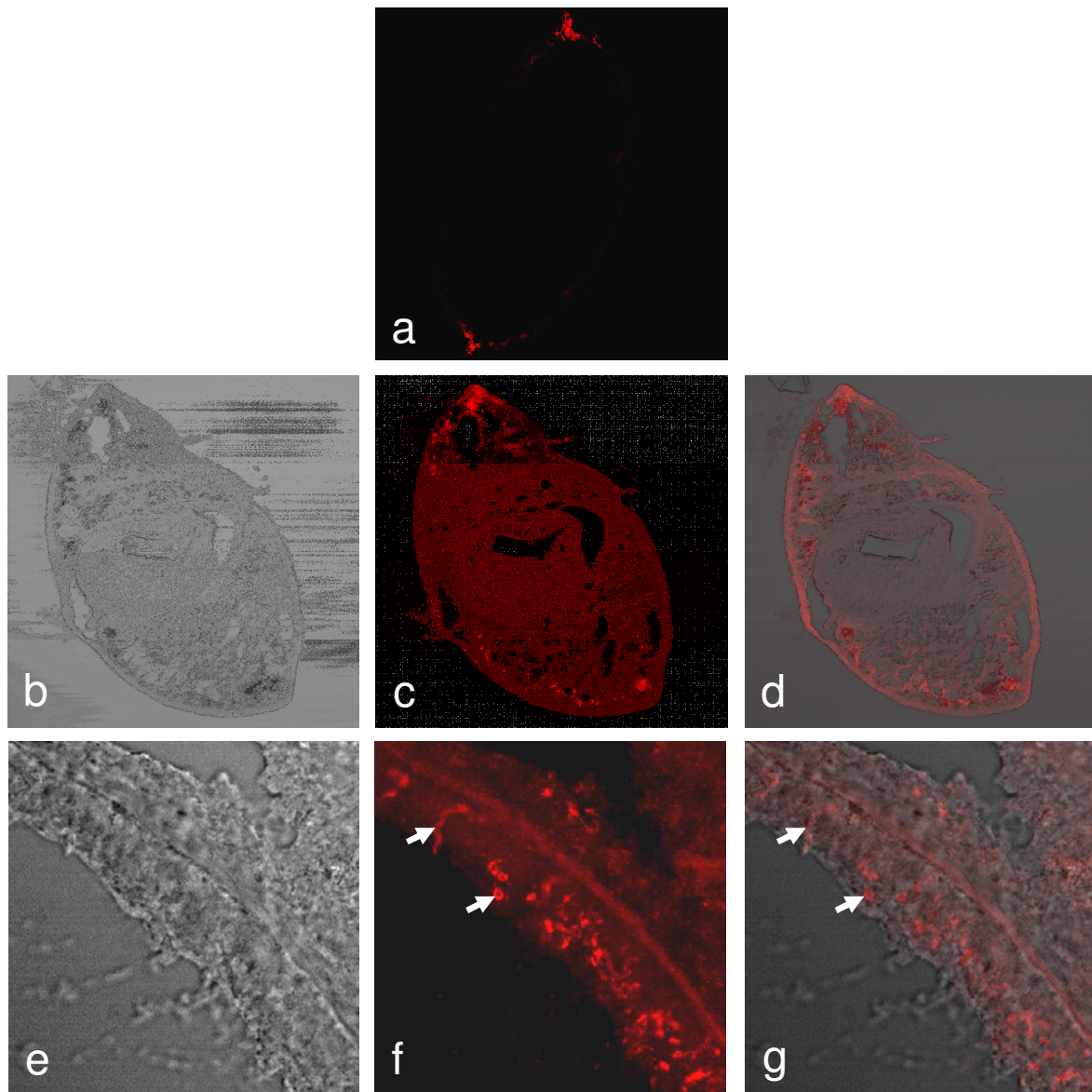


Figure 7

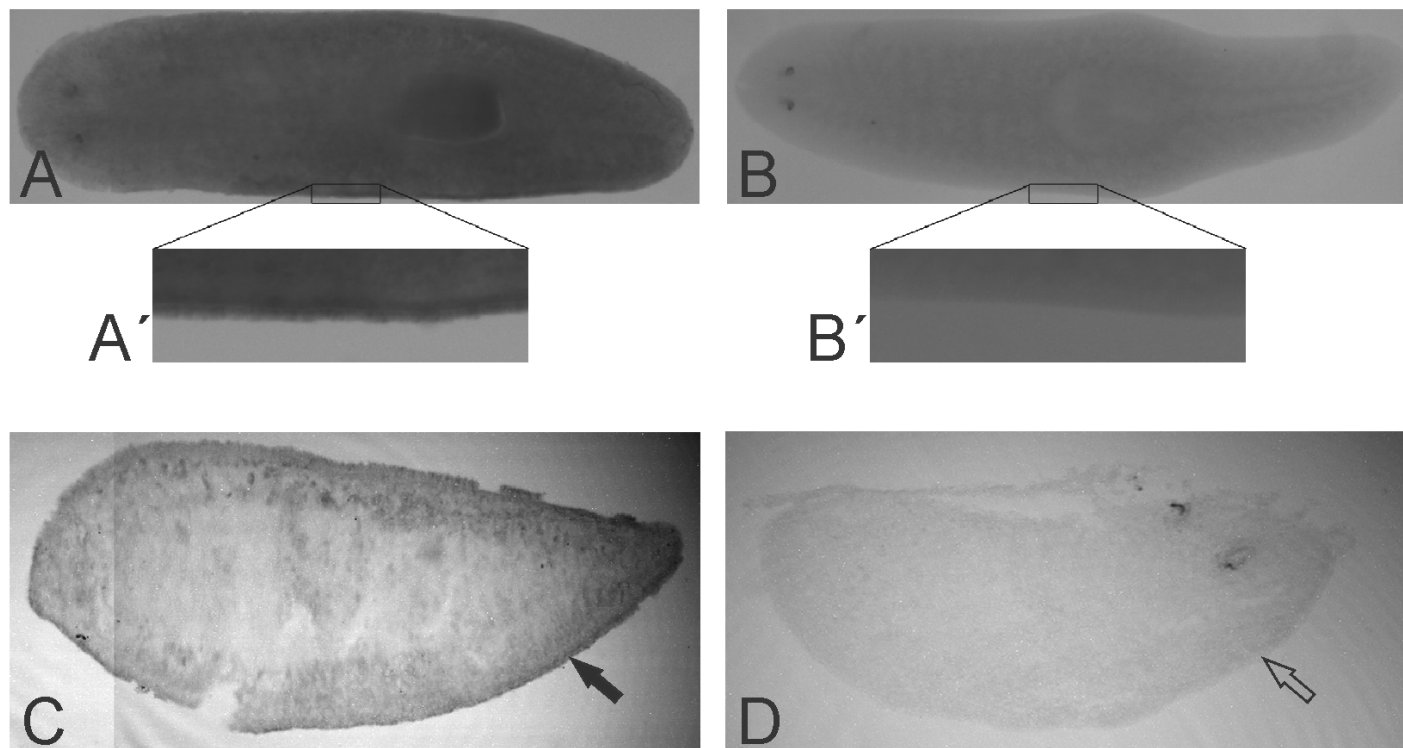


Figure 8

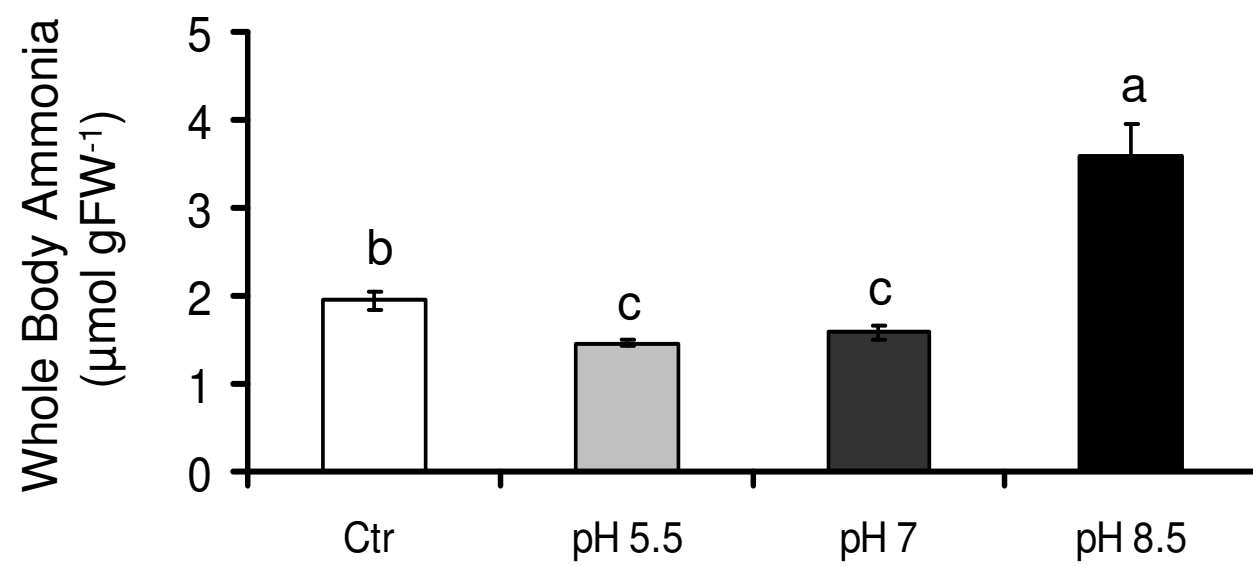


Figure 9

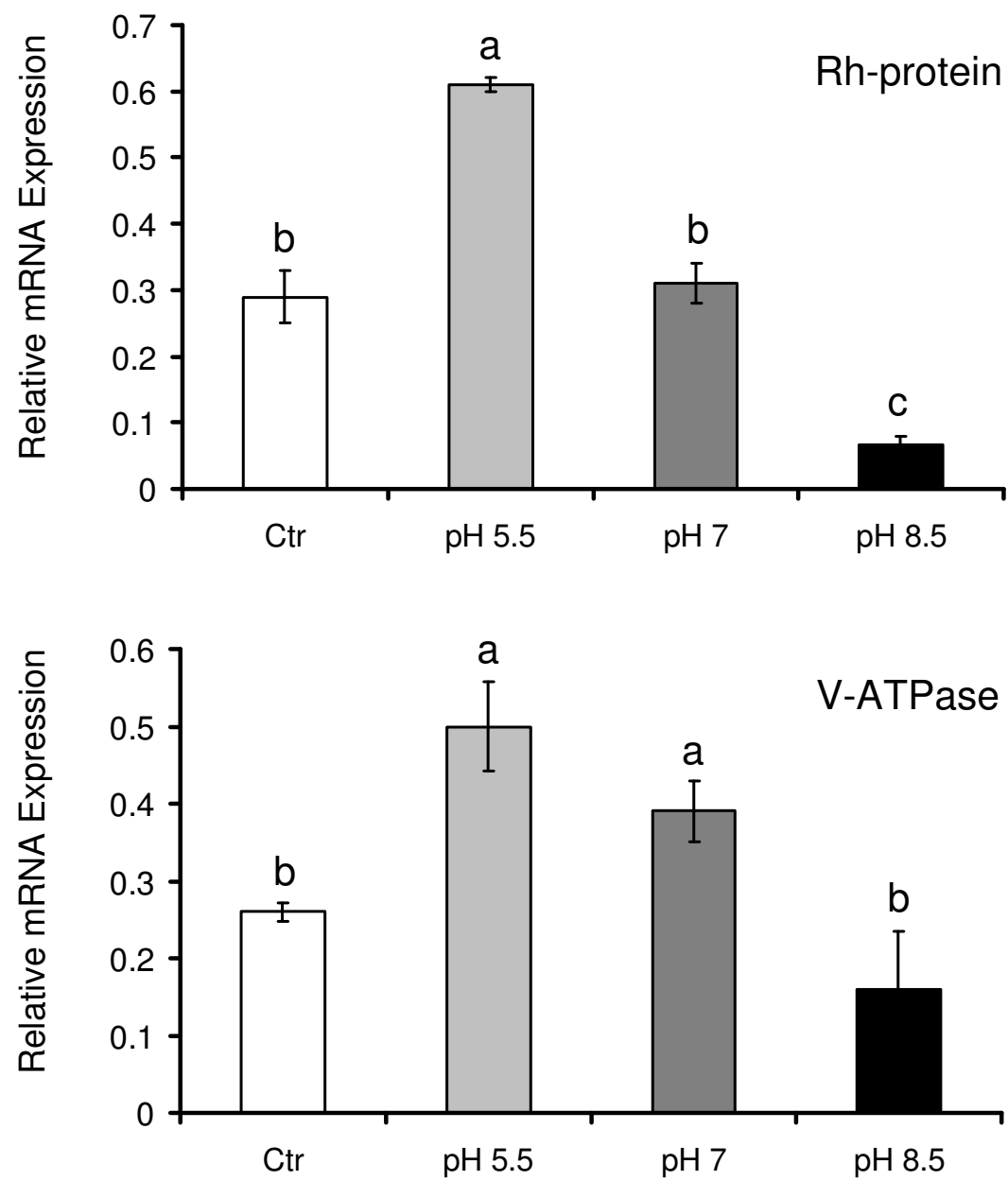


Figure 10

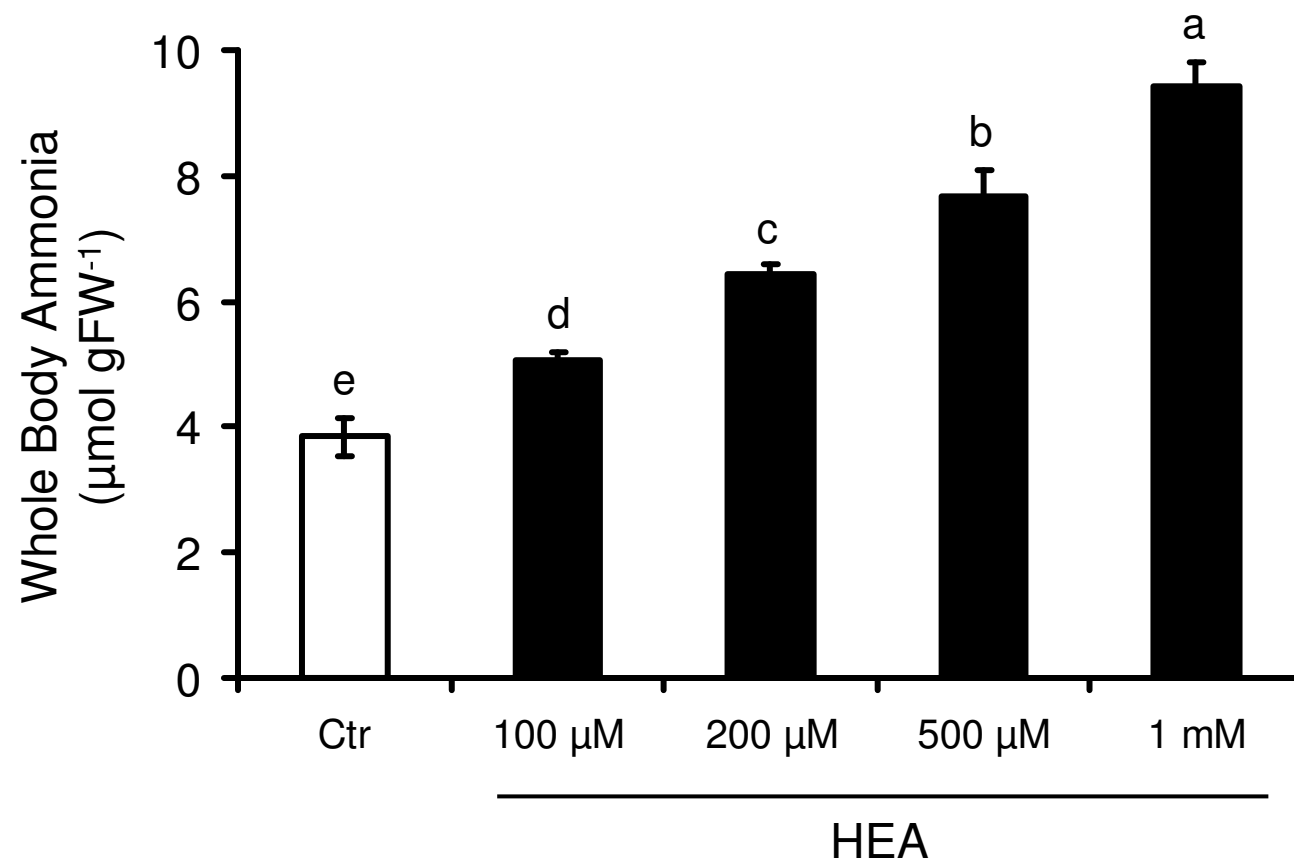


Figure 11

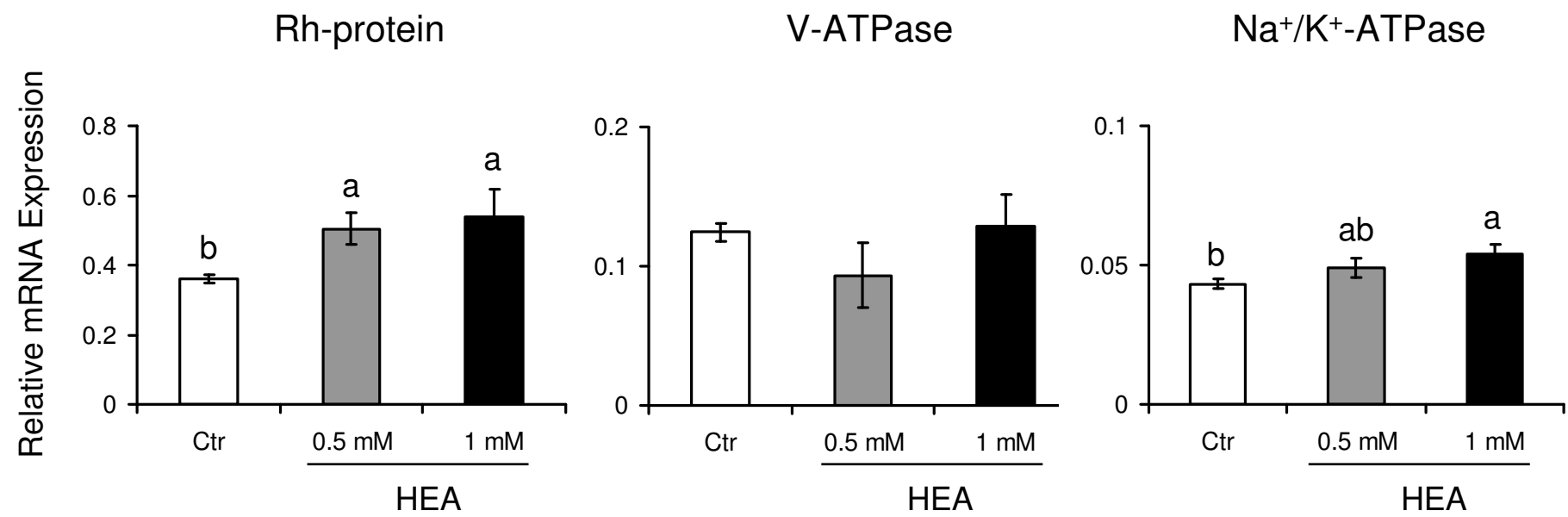


Figure 12

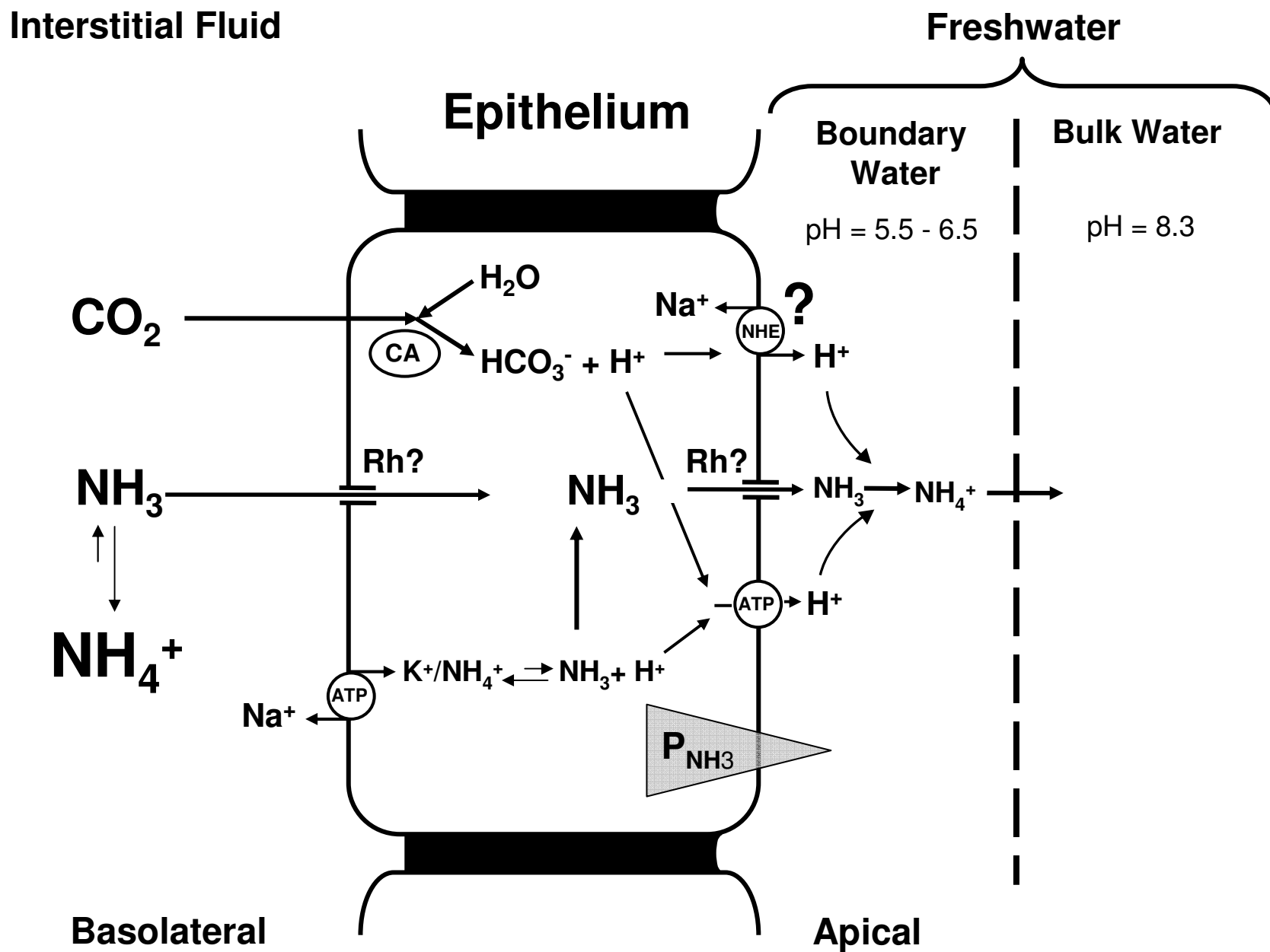


Figure 13